# DECOVALEX-2019
# Executive Summary

Bond A.E. and Birkholzer J.T.

With contributions from:
Armand G., Backers T., Gens A., Graupner B., Guglielmi Y., Harrington J.F., Rutqvist J., Iwatsuki, T., Meier T., Plúa C., Seyedi D., Shao H., Tamayo-Mas E., and Vitel M.

October 2020

DECOVALEX 2019

# Disclaimer

This document was prepared as an account of the international research project DECOVALEX-2019 comprising participants from industry, government and academia, with funding organizations--Andra, BGR/UFZ, CNSC, U.S. DOE, ENSI, JAEA, IRSN, KAERI, NWMO, RWM, SÚRAO, SSM and Taipower. The statements made in the report are, however, solely those of the authors and do not necessarily reflect those of the Funding Organizations. While this document is believed to contain correct information, neither the United States Government nor any agency thereof, nor the Regents of the University of California, nor any of their employees, makes any warranty, express or implied, or assumes any legal responsibility for the accuracy, completeness, or usefulness of any information, apparatus, product, or process disclosed, or represents that its use would not infringe privately owned rights. Reference herein to any specific commercial product, process, or service by its trade name, trademark, manufacturer, or otherwise, does not necessarily constitute or imply its endorsement, recommendation, or favoring by the United States Government or any agency thereof, or the Regents of the University of California. The views and opinions of authors expressed herein do not necessarily state or reflect those of the United States Government or any agency thereof or the Regents of the University of California.

# Copyright

This publication has been composed under the direction of editors at Lawrence Berkeley National Laboratory under Contract No. DE-AC02-05CH11231 with the U.S. Department of Energy, and Quintessa Limited, Birchwood, Warrington WA3 7QU, UK. The U.S. Government retains a non-exclusive, irrevocable, worldwide license to publish or reproduce this published report, or allow others to do so, for U.S. Government purposes.

# DECOVALEX-2019

# Executive Summary

**Lead Authors:**

Bond A.E. and Birkholzer J.T.
Quintessa Ltd and LBNL

**Contributing Authors (by organization):**

Tamayo-Mas E. and Harrington J.F.
British Geological Survey, Keyworth, Nottingham, United Kingdom

Graupner B.[1], Rutqvist J.[2], Guglielmi Y.[2]
[1]Swiss Federal Nuclear Safety Inspectorate (ENSI), Switzerland; [2]Lawrence Berkeley National Laboratory (LBNL), USA

Iwatsuki, T.
Japan Atomic Energy Agency

Gens A.
CIMNE_UPC

Plúa C.[1], Vitel M.[1], Seyedi D.[2] and Armand G.[1]
[1]Andra, France, [2]now at CEA, France

Shao H.
Federal Institute for Geosciences and Natural Resources (BGR), Germany

Meier T. and Backers T.
geomecon GmbH, Germany

October 2020

**LBNL- 2001360**

# Preface

The DECOVALEX Project is an on-going international research collaboration, established in 1992, to advance the understanding and modeling of coupled Thermal (T), Hydrological (H), Mechanical (M) and Chemical (C) processes in geological in geological systems. DECOVALEX was initially motivated by the recognition that prediction of these coupled effects is an essential part of the performance and safety assessment of geologic disposal systems for radioactive waste and spent nuclear fuel. Later it was realized that these processes also play a critical role in other subsurface engineering activities, such as subsurface $CO_2$ storage, enhanced geothermal systems, and unconventional oil and gas production through hydraulic fracturing. Research teams from many countries (e.g., Canada, China, Czech Republic, Finland, France, Germany, Japan, Republic of Korea, Spain, Sweden, Switzerland, Taiwan, United Kingdom, and the United States) various institutions have participated in the DECOVALEX Project over the years, providing a wide range of perspectives and solutions to these complex problems. These institutions represent radioactive waste management organizations, national research institutes, regulatory agencies, universities, as well as industry and consulting groups.

At the core of the collaborative work with in DECOVALEX is the collaborative analysis and comparative modeling of state-of-the-art field and laboratory experiments. DECOVALEX engages model comparison in a broad and comprehensive sense, including the modelers' interpretation of experimental data, selection of boundary conditions, rock and fluid properties, etc., in addition to their choice of coupling schemes and simulator. In-depth and detailed discussions among the teams yield insight into the coupled THMC processes and stimulate development of modeling capabilities and measurement methods which would not be possible if the data were studied by only one or two groups.

Since the project initiation, DECOVALEX has been organized in several four-year phases, each phase featuring a number of modeling tasks of importance to radioactive waste disposal and other geoscience applications. Six project phases were successfully concluded between 1992 and 2015, results of which have been summarized in several overview publications (e.g., Tsang et al., 2009; Birkholzer et al., 2018; Birkholzer et al., 2019). The most recent phase, named DECOVALEX-2019, started in 2016 and ended in 2019. Seven tasks were conducted in DECOVALEX-2019, as follows:

- **Task A: ENGINEER** - Advective gas flow through low permeability materials
- **Task B: Fault Slip Test** - Fault slip processes in argillaceous rock
- **Task C: GREET** - Hydro-mechanical-chemical processes during groundwater recovery
- **Task D: INBEB** - HM and THM interactions in bentonite engineered barriers
- **Task E: Upscaling Heater Tests** - Upscaling of heater test results to repository scale
- **Task F: FINITO** - Fluid inclusions and movement in tight rock
- **Task G: EDZ Evolution** - EDZ evolution and permeability changes in crystalline rock

The DECOVALEX Project would not have been possible without the support and engagement from the participating organizations who jointly support coordination of the project within a given project phase, propose and coordinate modeling tasks including the necessary experimental data, and deploy their own research team (or teams) working on a selection of the tasks conducted in the project. The partner organizations in DECOVALEX-2019 were:

- Andra, National Radioactive Waste Management Agency, *France*
- BGR, Federal Institute for Geosciences and Natural Resources, *Germany*
- CNSC, Canadian Nuclear Safety Commission, *Canada*
- DOE, Department of Energy, *USA*
- ENSI, Swiss Federal Nuclear Safety Inspectorate, *Switzerland*
- IRSN, Institut de Radioprotection et de Sûreté Nucléaire, *France*
- JAEA, Japan Atomic Energy Agency, *Japan*
- KAERI, Korea Atomic Energy Research Institute, Republic of Korea
- NWMO, Nuclear Waste Management Organization, *Canada*
- RWM, Radioactive Waste Management, *United Kingdom*
- SSM, Swedish Radiation Safety Authority, *Sweden*
- SÚRAO, Radioactive Waste Repository Authority, *Czech Republic*
- Taipower, Taiwan Power Company, *Taiwan*
- UFZ, Helmholtz Centre for Environmental Research, *Germany*

We are extremely grateful to these organizations for their financial and technical support of DECOVALEX-2019.

*Jens Birkholzer (Chairman of the DECOVALEX project) and Alex Bond (Technical Coordinator of the DECOVALEX Project).*

*Berkeley, California, USA, October 2020*

**References:**

Birkholzer, J.T., Bond, A.E., Hudson, J.A., Jing, L., Tsang, C.-F., Shao, H., Kolditz, O. (2018): DECOVALEX-2015 - An International Collaboration for Advancing the Understanding and Modeling of Coupled Thermo-Hydro-Mechanical-Chemical (THMC) Processes in Geological Systems, Environmental Earth Sciences, 77(14).

Birkholzer, J.T., Tsang, C.-F., Bond, A.E., Hudson, J.A., Jing, L., and Stephansson, O. (2019): 25 Years of DECOVALEX - Scientific Advances and Lessons Learned from an International Research Collaboration in Coupled Subsurface Processes, Invited Review, International Journal and Rock Mechanics and Mining Sciences, 122.

Tsang, C.-F., Stephansson, O., Jing, L., and Kautsky, F. (2009): DECOVALEX Project: from 1992 to 2007. Environmental Geology, 57(6).

# Contents


**1 Introduction 1**

1.1 Background and Objectives 1

1.2 Organization 2

**2 Task A – modElliNg Gas INjEction expERiments (ENGINEER) 6**

2.1 Background and Motivation 6

2.2 Organization and Participation 7

2.3 Experimental Data 7

2.4 Task Approach and Selected Results 10

2.5 Key Outcomes 14

2.6 Outstanding Issues 15

2.7 Future Work 15

**3 Task B – Fault Slip Experiment 17**

3.1 Background and Motivation 17

3.2 Organization and Participation 17

3.3 Experimental Data 18

3.4 Task Approach and Selected Results 19

3.5 Key Outcomes 24

3.6 Outstanding Issues 24

3.7 Future Work 25

**4 Task C – Groundwater REcovery Experiment in Tunnel (GREET) 26**

4.1 Background and Motivation 26

4.2 Organization and Participation 27

4.3 Experimental Data 28

4.4 Task Approach and Selected Results 29

4.5 Key Outcomes 33

4.6 Outstanding Issues 34

**5 Task D – Hydro-Mechanical Interactions in Bentonite Engineered Barriers (INBEB) 35**

5.1 Background and Motivation 35

5.2 Experimental Data 35

5.3 Participation and Organization 37

5.4 Task Approach and Selected Results 38

5.5 Key Outcomes 42

5.6 Outstanding Issues 42

**6 Task E – Upscaling of Modelling Results from One-to-one to Field Scale 43**
6.1 Background and Motivation 43
6.2 Organization and Participation 43
6.3 Experimental Data 44
6.4 Task Approach and Selected Results 47
6.5 Key Outcomes 50
6.6 Outstanding Issues 51
6.7 Future Work 51

**7 Task F – Fluid Inclusion and Modelling in Tight Rock (FINITO) 52**
7.1 Background and Motivation 52
7.2 Organization and Participation 53
7.3 Task Approach and Selected Results 54
7.4 Key Outcomes 55
7.5 Outstanding Issues 56

**8 Task G - EDZ Evolution in Sparsely Fractured Competent Rock 57**
8.1 Background and Motivation 57
8.2 Organization and Participation 58
8.3 Experimental Data 58
8.4 Task Approach and Selected Results 60
8.5 Key Outcomes 62
8.6 Outstanding Issues 63
8.7 Future Work 63

**9 Concluding Remarks 64**
9.1 Novel Representations of Complex Processes 64
9.2 Complexities of Fracture Representation 65
9.3 Complex Hydro-Mechanics with Wider Applications 65
9.4 THM Processes in Clays 66
9.5 Overall Comments 67

**10 Acknowledgements 69**

**11 References 70**

# 1 Introduction

## 1.1 Background and Objectives

The international co-operative research project, DECOVALEX-2019 project (2016-2019), is the 7th phase of the long-running DECOVALEX project starting in 1992. Previous phases were DECOVALEX I (1992-1995), DECOVALEX II (1996-1999), DECOVALEX III (2000-2003), DECOVALEX-THMC (2004-2007), DECOVALEX-2011 (2008-2011) and DECOVALEX-2015 (2012-2015). The project was initiated as a multi-disciplinary interactive and co-operative research effort for understanding and modelling coupled thermo-hydro-mechanical-chemical (T-H-M-C) processes of geological media and systems for supporting performance assessment (PA) and safety assessment (SA) of repositories for geological disposal of radioactive wastes. The motivations for such long-term international co-operation are to jointly improve basic understanding of the coupled THMC processes of importance for radionuclide release and transport, to provide a forum for regular international peer reviews, information exchanges and developments of experimental experiences and developments of mathematical modelling methods and computer codes. The history of the project has shown that this kind of international co-operation provides also an efficient platform for exchanging extensive and valuable laboratory and in-situ experimental data for model/code verifications, demonstrating the current state-of-the-science of the coupled T-H-M-C issues for nuclear waste repository performance assessment, and educating young research students.

The overall aim of DECOVALEX-2019 was to increase the understanding of various thermo-hydro-mechanical-chemical processes of importance for radionuclide release and transport from a repository to the biosphere and how they can be described and modelled using mathematical models. The scientific and technical objectives are: to increase the basic understanding of T-H-M-C coupled processes in fractured rocks (crystalline, sedimentary, argillaceous) and buffer materials; to investigate the predictive capabilities of different codes to field experiments and to perform verification of codes; to exchange experimental data, and improve the understanding of the constitutive behavior of crystalline and argillaceous rock masses and buffer materials; and to perform THMC calculations in a performance/safety assessment context.

Seven tasks were conducted in DECOVALEX-2019, as follows:

- Task A: ENGINEER - Advective gas flow through low permeability materials
- Task B: Fault Slip Test - Fault slip processes in argillaceous rock
- Task C: GREET - Hydro-mechanical-chemical processes during groundwater recovery
- Task D: INBEB - HM and THM interactions in bentonite engineered barriers
- Task E: Upscaling Heater Tests - Upscaling of heater test results to repository scale
- Task F: FINITO - Fluid inclusions and movement in tight rock
- Task G: EDZ Evolution - EDZ evolution and permeability changes in crystalline rock

DECOVALEX will continue in a new phase 'DECOVALEX-2023' comprising seven exciting tasks covering a wide range of spatial and temporal scales. For the first time the project will include a full performance assessment benchmarking exercise, and a field experiment in bedded salt using data from the Salt Heater Test at the Waste Isolation Pilot Plant, USA.

## 1.2 Organization

The DECOVALEX-2019 project consists of thirteen funding organizations (FO) as listed in Table 1, a Management Organization (Lawrence Berkeley National Laboratory), a Chair (Jens Birkholzer – LBNL) and a Technical Coordinator (Alex Bond – Quintessa Ltd). Funding organizations provide financial support for the project organization and they support research teams that may participate in one or more of the tasks. Some funding organizations also propose and lead a task, in which case they will provide funding for the task leader. In DECOVALEX-2019, five of the seven tasks were directly led by a funding organization (Tasks B, C, E, F, and G; see Table 2). In two cases (Tasks A and D), the funding for task leaders was provided by the DECOVALEX Project as these were tasks of high scientific interest, but lacked a specific funding organization to provide the task management.

Table 2 shows the Research Teams, their respective funders and tasks in which they participated. Figure 1 shows the flowchart of the project organization.

**Table 1. Summary of Funding Organizations in DECOVALEX-2019.**

| Funding Organization | Full Name | Country |
|---|---|---|
| **ANDRA** | l'Agence nationale pour la gestion des déchets radioactifs | France |
| **BGR/UFZ** | Federal Institute for Geosciences and Natural Resources (BGR) Helmholtz Centre for Environmental Research (UFZ) | Germany |
| **CNSC** | Canadian Nuclear Safety Commission | Canada |
| **DOE** | U.S. Department of Energy, Office of Nuclear Energy | USA |
| **ENSI** | Swiss Federal Nuclear Safety Inspectorate | Switzerland |
| **JAEA** | Japan Atomic Energy Agency | Japan |
| **KAERI** | Korea Atomic Energy Research Institute | Korea |
| **NWMO** | Nuclear Waste Management Organization | Canada |
| **RWM** | Radioactive Waste Management | UK |
| **SÚRAO** | Správa úložišť radioaktivních odpadů | Czech Republic |
| **IRSN** | Institut de Radioprotection et de Sûreté Nucléaire | France |
| **SSM** | Strålsäkerhetsmyndigheten (Swedish Radiation Safety Authority) | Sweden |
| **TaiPower** | Taiwan Power Company | Taiwan |

**Table 2. Summary of Funding Organizations and Research Teams for each task. Entries in brackets indicate limited participation. Task leader organizations highlighted in blue are centrally funded by the DECOVALEX project. Note that IRSN ultimately did not participate in any tasks.**

| Funding Organization | Task A | Task B | Task C | Task D | Task E | Task F | Task G |
|---|---|---|---|---|---|---|---|
| ***Task Lead Organization*** | ***BGS*** | ***ENSI*** | ***JAEA*** | ***CIMNE-UPC*** | ***ANDRA*** | ***BGR/UFZ*** | ***SSM*** |
| **BGR/UFZ** | BGR/UFZ | BGR/UFZ | | | UFZ/BGR | BGR/UFZ | |
| **DOE** | SNL and LBNL | LBNL | SNL | | LBNL | SNL | (SNL) |
| **ENSI** | | ENSI | | | | | |
| **JAEA** | | | JAEA | JAEA | | | |
| **KAERI** | KAERI | KIGAM | | KAERI | | | |
| **RWM** | Quintessa | | | | Quintessa | | |
| **SÚRAO** | | | TUL | IGN | | | TUL/IGN |
| **IRSN** | | | | | | | |
| **CNSC** | CNSC | CNSC | | | | | |
| **SSM** | | DynaFrax | | | | | Geomecon and SNU |
| **ANDRA** | CIMNE-UPC | | | | ANDRA | | |
| **TaiPower** | NCU/TP | INER | | NCU/TP | | | |
| **NWMO** | | | | | NWMO | | |

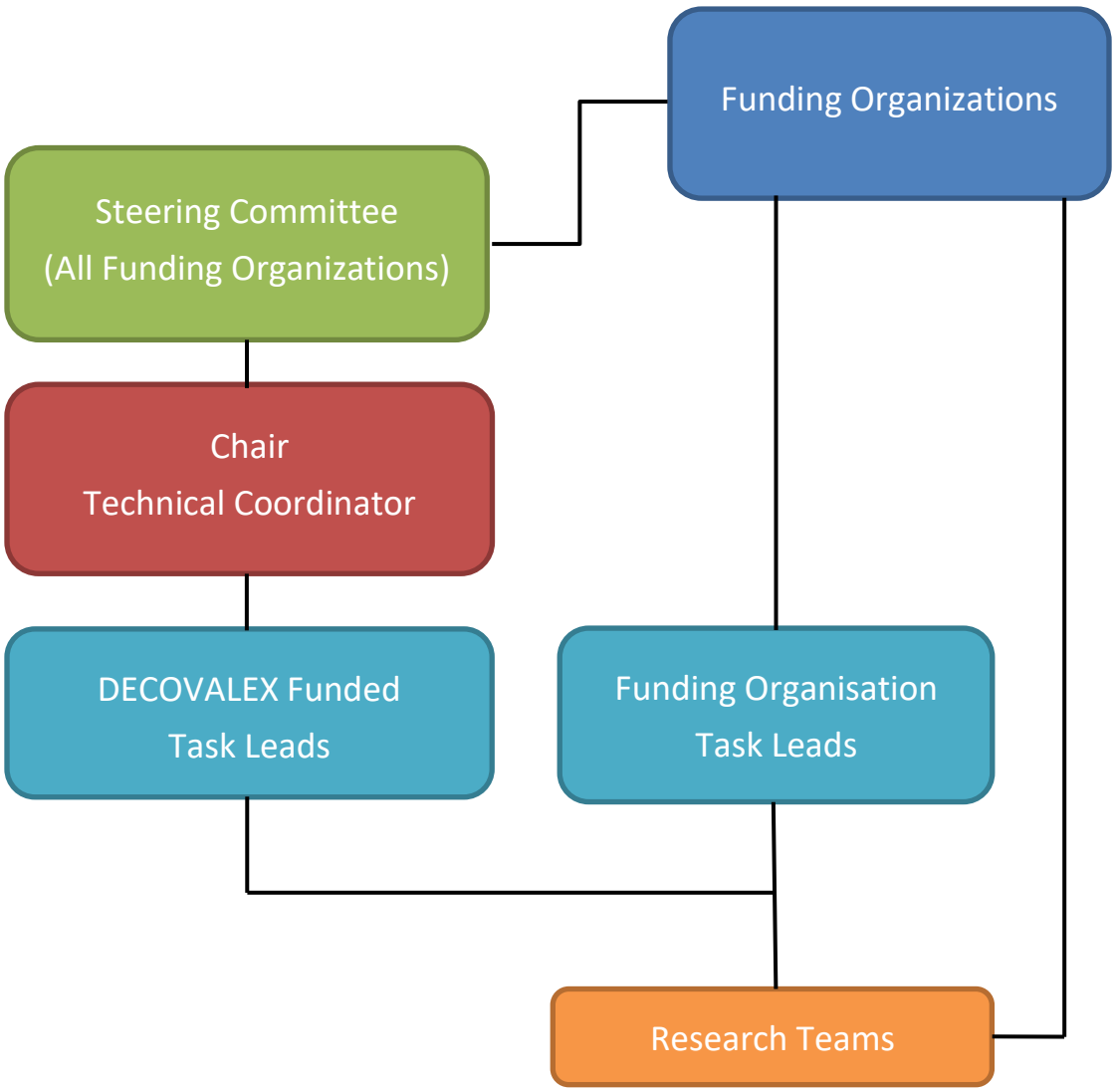


**Figure 1. Organization flowchart for DECOVALEX-2019 project.**

# 2 Task A – modElliNg Gas INjEction expERiments (ENGINEER)

## 2.1 Background and Motivation

In a repository for radioactive waste hosted in low permeability formations, hydrogen and other gases may be generated due to the corrosion of metallic materials, the radioactive decay of waste and the radiolysis of water. If the gas production rate exceeds the gas diffusion rate within the pores of the host rock formation, a discrete gas phase will form and accumulate until its pressure becomes large enough to exceed the entry pressure of the surrounding material, at which point dilatant, advective flow of gas is expected to occur.

The purpose of Task A is to better understand the processes governing the advective movement of gas in both low-permeability argillaceous repository host rocks and clay-based engineered barriers. Special attention is given to the mechanisms controlling gas entry, flow and pathway sealing and their impact on the performance of the engineered clay barrier (Figure 2).

Previous work suggests gas flow may be accompanied by the creation of dilatant pathways whose properties change temporally and spatially within the medium. Thus, new numerical representations for the quantitative prediction of gas migration fluxes through argillaceous rock formations have been developed. These provide an invaluable tool with which to assess the impact of gas flow on repository layout and therefore design of any future facility. In addition, experience gained through this task is of direct relevance to other clay-based engineering issues where immiscible gas flow is a consideration including shale gas, hydrocarbon migration, carbon capture and storage and landfill design.

Full details of the work are summarised by Tamayo-Mas and Harrington (2020).

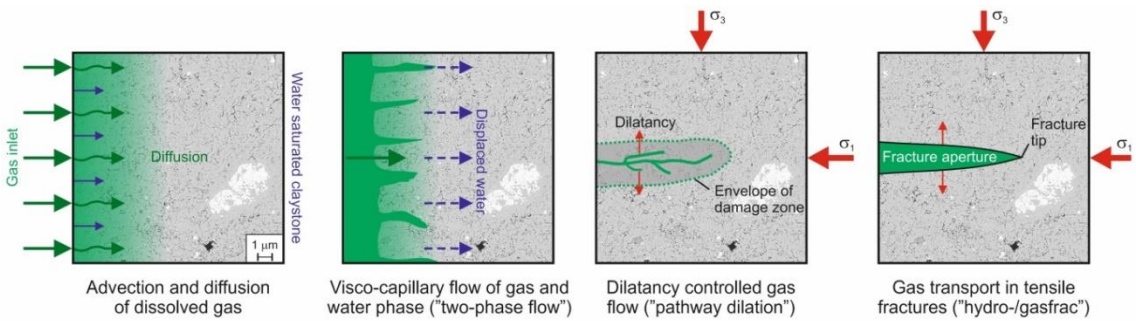


**Figure 2. Conceptual models of gas flow (after Marschall et al. 2005), BGS © UKRI.**

## 2.2 Organization and Participation

Task A was organised into three steps, starting with code development (stage 0), followed by modelling of a 1D gas flow test (stage 1) and a 'spherical' gas flow test (stage 2). An optional stage (stage 3), dealing with natural argillaceous materials, was also introduced but only modelled by a single team.

1. BGR/UFZ (Germany): Federal Institute for Geosciences and Natural Resources and the Helmholtz Centre for Environmental Research.
2. CNSC (Canada): Canadian Nuclear Safety Commission.
3. KAERI (Korea): Korea Atomic Energy Research Institute.
4. LBNL (United States of America): Lawrence Berkeley National Laboratory.
5. NCU/TPC (Taiwan): National Central University and Taiwan Power Company (Taipower).
6. Quintessa/RWM (United Kingdom): Quintessa Ltd on behalf of Radioactive Waste Management.
7. SNL (United States of America): Sandia National Laboratories.
8. CIMNE-UPC/Andra (Spain/France): Universitat Politècnica de Catalunya, funded by l'Agence nationale pour la gestion des déchets radioactifs.

## 2.3 Experimental Data

Two different experiments undertaken by the British Geological Survey (BGS) were used in this task. The first one (stage 1) consisted of a 1D gas injection test performed on a compacted bentonite sample (119.88 mm length x 59.59 mm diameter) supplied by Clay Technology AB (Lund, Sweden) and prepared by BGS. See Daniels and Harrington (2017)

for a detailed description of the sample preparation and Harrington and Horseman (2003) for a general description of the experimental apparatus. The second experiment (stage 2) consisted of a spherical gas injection test performed on a compacted bentonite sample (119.88 mm length x 59.59 mm diameter), also supplied by Clay Technology AB and prepared by BGS; see Harrington et al. (2017) for further detail. A key difference between the 1D and spherical injection tests is the outflow for the spherical flow case is via three isolated ports on the radial outer surface rather than across an single continuous end-plate. Both tests are comprised of two stages; hydration followed by gas testing. During these two stages, stresses and pore pressures were continuously monitored and used by the teams to assess their modelling strategies.

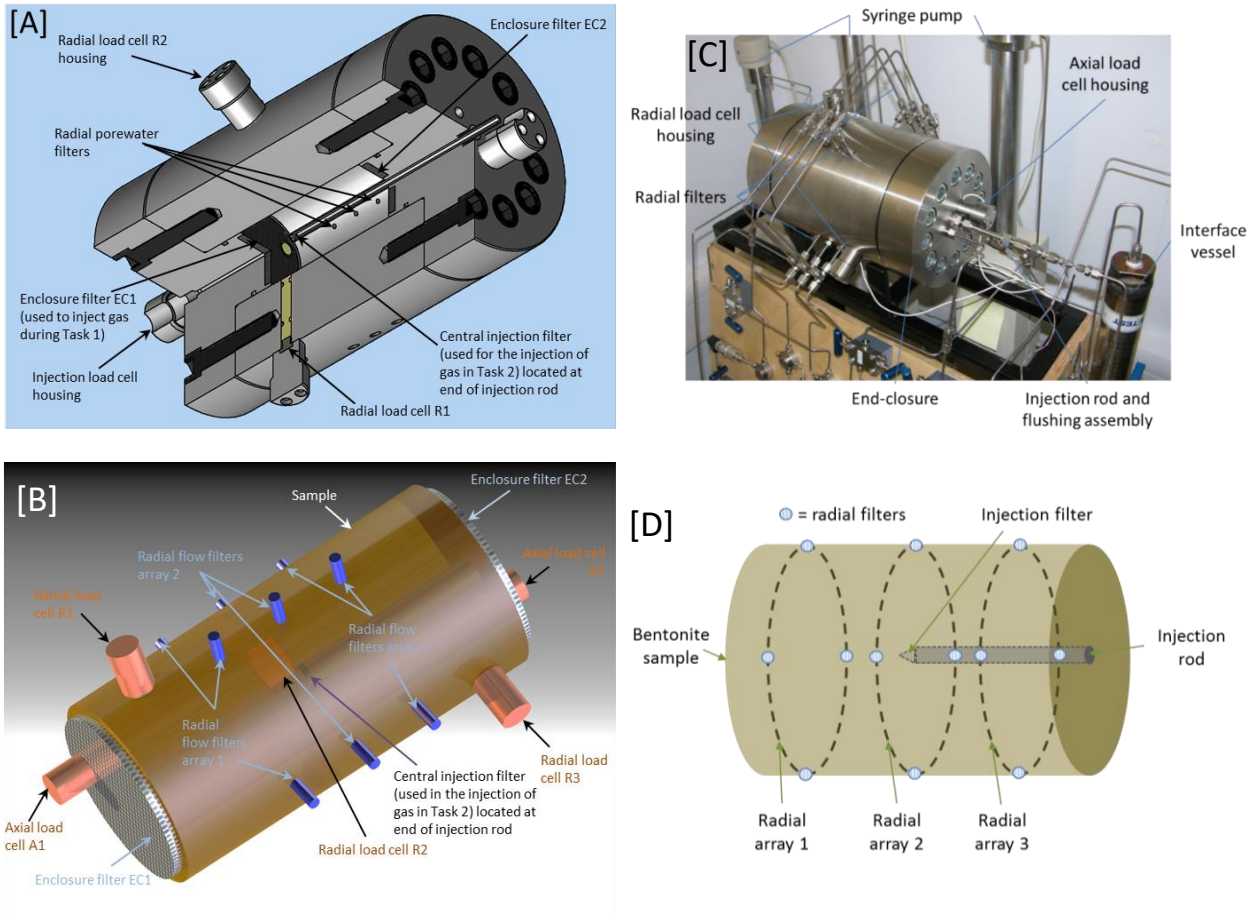


**Figure 3. [A-B] Cut-away schematic of the constant volume and radial flow (CVRF) gas migration apparatus used in this study from two perspectives showing the instrumentation. Note filters/load cells on the back of the vessel are not visible in these drawings. [C] Photograph of apparatus and tubing connections. [D] Schematic showing the location of the central gas injection filter and radial drainage arrays. Sample dimensions are nominally 120 mm in length and 60 mm in diameter. From Tamayo-Mas and Harrington (2020).**

Both tests had a progressive increase pressure through the injector assembly, followed by one or more breakthrough events from the injector to one or more outflow locations. For stage 1 post breakthrough a shut-in enforced (71 days - Figure 4), while for stage 2 continuous gas flow is maintained post injection.

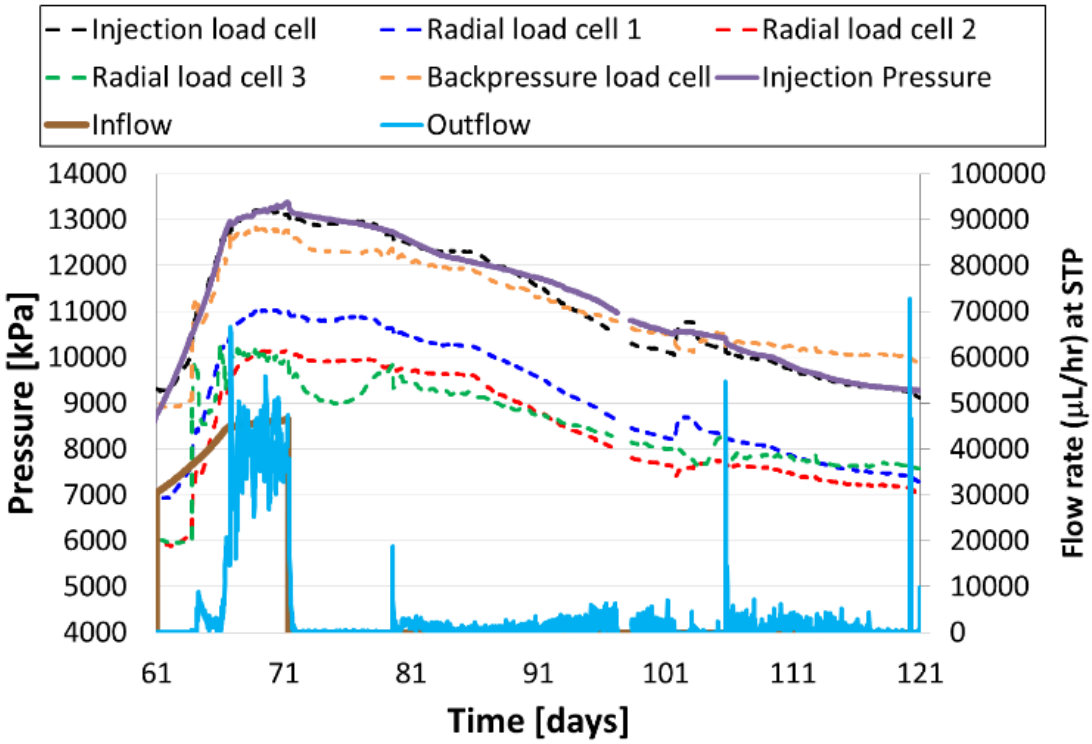


**Figure 4. Stage 1: total stress and flow data from day 61 to day 121. Standard temperature and pressure (STP) are defined as 273.15 K and 101.325 kPa respectively. Note that 'Inflow' is the gas compression rate within the injection system rather than gas inflow into the sample.**

Stage 3 considered a 1D experiment with a constant radial load rather than being a constant volume test, but critically using a COx argillite sample rather than compacted bentonite. The experimental results are complex and only a single team attempted this stage see Annex A of Tamayo-Mas and Harrington (2020).

## 2.4 Task Approach and Selected Results

Four types of approaches have been developed to model the movement of gas in the above-mentioned 1D and 3D experiments: (i) standard two-phase flow models incorporating a range of different mechanical deformation behaviors, (ii) enhanced two-phase flow models in which fractures are embedded within a plastic material (continuous techniques) or incorporated into the model using a rigid-body-spring network (discrete approaches), (iii) a single-phase model incorporating a creep damage function in which only gas flow is considered, and (iv) a conceptual approach used to examine the chaotic nature of gas flow. The codes and approaches used are summarized in Table 3.

The experimental data from these gas injection tests exhibit a combination of stochastic and deterministic behaviors. Both breakthrough after a period of increasing gas pressure, and bulk gas flow through a main emergent pathway are common to the 1D and 3D experiments (e.g. Figure 5). The instability and pathway switching observed in the 3D experiment before a main flow path is established suggests that the precise timing of the gas breakthrough and associated gas flows may be stochastic by nature. It is therefore important for modelers to understand and distinguish between the key experimental features reproducible across all experiments and those that only occur in specific experiments. It is also important to recognize that different modelling approaches have different objectives in terms of their intended application. The results of models need to be judged against their stated objectives rather the full detail of the experiments, the specifics of which may or may not be significant for the application. Even simple models can have an intrinsic value and can also give insights into the phenomenological behavior exhibited in the experiments.

Example results showing the radial stresses calculated for models for stage 1 are shown in Figure 6. The variation in results in the early part of the modelling reflect differing approaches in representing the sample saturation – some teams modelled it explicitly while others simply took reference conditions and started the evolution at injection start. Greater variation is shown in the calculated stage 1 gas outflow rates where many teams noticeably struggled to replicate the constant flow post breakthrough, followed by rapid shutdown of flows as injection halts (Figure 7).

**Table 3. Modelling approaches and codes that have been used during Task A**

| Model | Funding Organization | Code | Kind of model | Mechanical deformation | Hydraulic approach |
|---|---|---|---|---|---|
| BGR/UFZ-E | BGR/UFZ | OpenGeoSys | continuous | elasticity | two phases |
| CNSC-PD | CNSC | COMSOL Multiphysics® | continuous | elastoplastic damage | two phases |
| KAERI-D | KAERI | Stage 1: TOUGH2 / FLAC3D<br>Stage 2: COMSOL Multiphysics® | continuous | elastic damage model | two phases |
| NCU/TPC-V | Taiwan Power Company | THMC | continuous | visco-elastic | two phases |
| CIMNE-UPC/ Andra-ED | ANDRA | Code_bright | continuous | elasticity with dilatancy | two phases with embedded fracture |
| LBNL-D | US DOE | TOUGH-RBSN | discontinuous | elastic-brittle damage and fractures | two phases |
| Quintessa/ RWM-ECap | RWM | QPAC | continuous | elasticity | single phase |

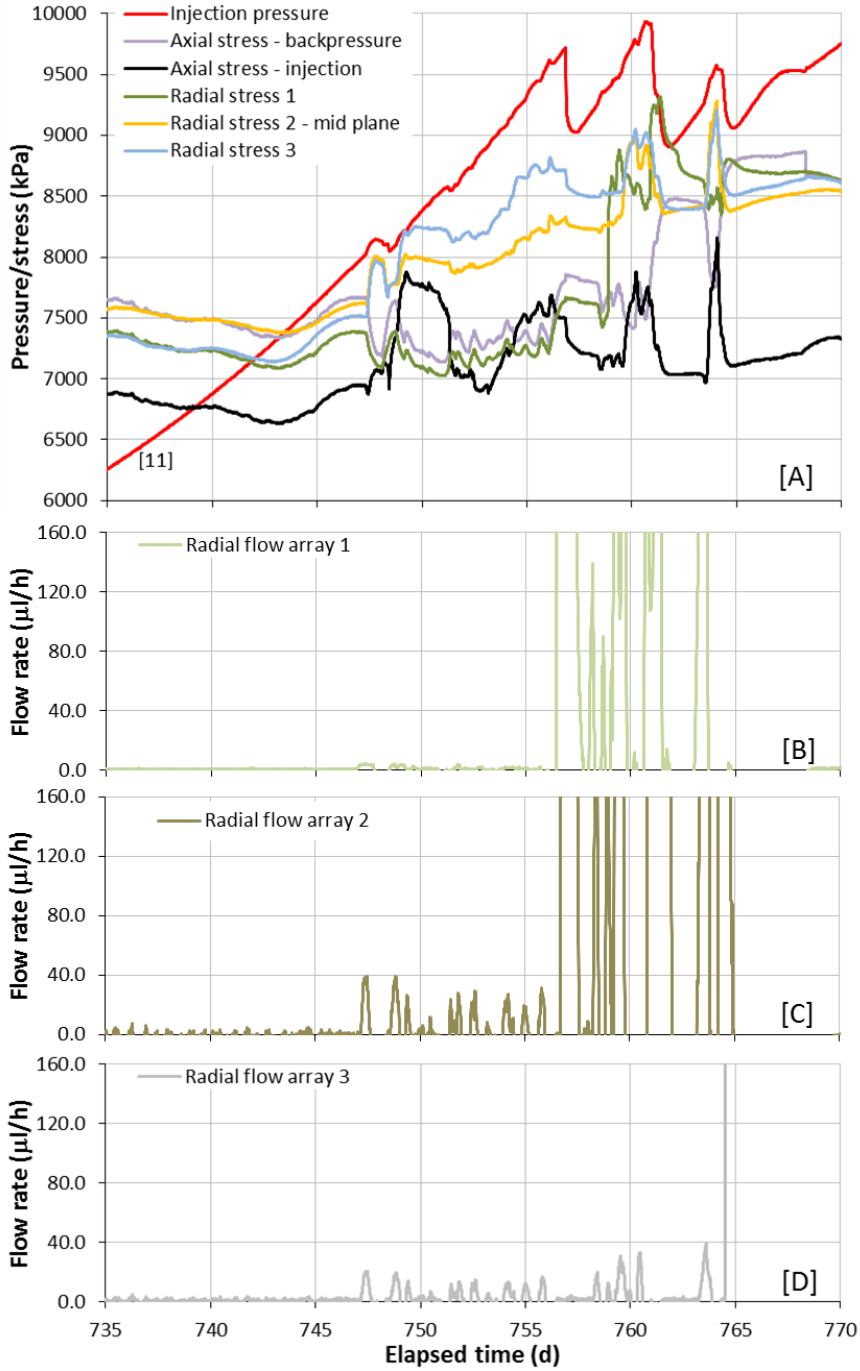


**Figure 5. Stage 1: evolution in gas pressure, stress and outflow during multiple gas breakthrough events. Graph [A] depicts gas pressure and local stress. [B], [C] and [D] show the outflow of gas (under experimental conditions) to radial arrays 1, 2 and 3 respectively. Inflections in stress are indicative of pathway propagation events and are often accompanied by outflow to one or more arrays (Figure 3). Major gas breakthrough events are noted around days 757, 761 and 764 signified by sudden drops in gas pressure, changes in the distribution of stress and the rapid discharge of gas. Outflow data is time-averaged to help identify underlying trends. This introduces a small time-shift in the data of ±3 h which explains why outflow appears to occur marginally before peak gas pressures. From Tamayo-Mas and Harrington (2020).**

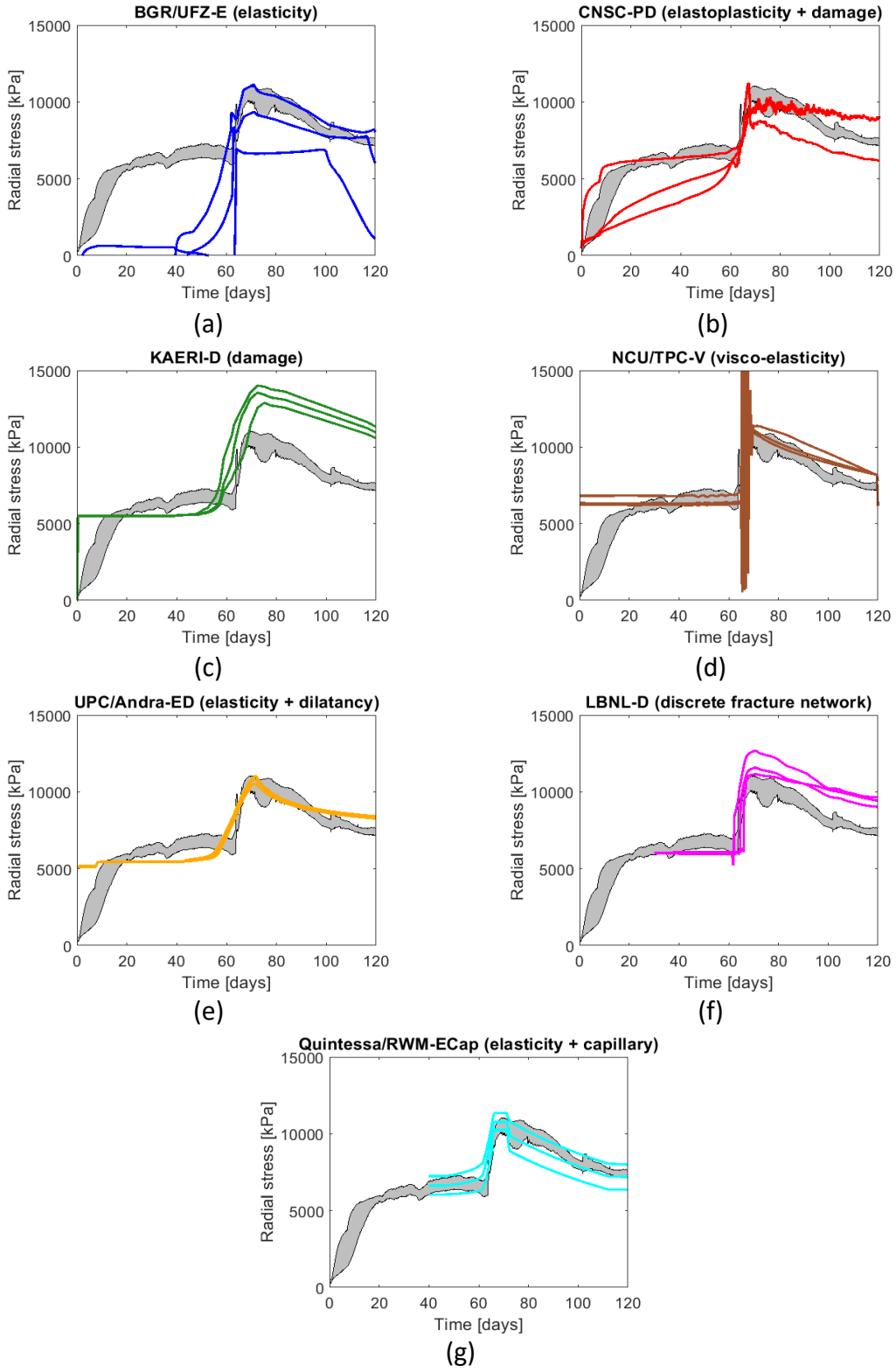


**Figure 6. Stage 1: experimental versus numerical radial stresses, obtained with models (a) BGR/UFZ-E, (b) CNSC-PD, (c) KAERI-D, (d) NCU/TPC-V, (e) CIMNE-UPC/Andra-ED, (f) LBNL-D and (g) Quintessa/RWM-ECap.**

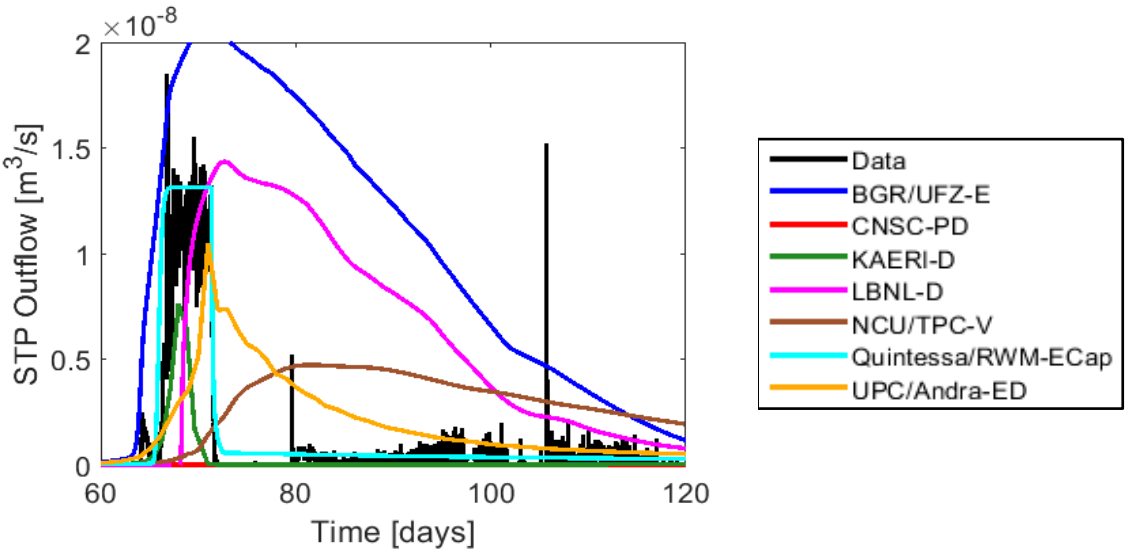


**Figure 7. Stage 1: comparison of modelled versus observed outflow results.**

## 2.5 Key Outcomes

Application of the numerical models shows that some continuous strategies are capable of obtaining a good fitting with respect to experimental stress measurement and bulk gas flow results. However, these models require substantial calibration of fitting parameters and focus on the deterministic features rather than representing the stochastic behavior observed in the experiments.

Continuous approaches with preferential pathways have fewer constraints within the models and while they are largely unable to represent some experimental details, the phenomenological processes are better represented. Similarly, discrete models, whose basis reflects the underlying physics of gas flow, also struggle to capture some of the key experimental features of the data such as stress or pore pressure distributions. Varying results are also observed in the prediction of bulk flow with different models performing well. While basic continuous strategies can provide some good fits to the data, it again reflects the higher level of calibration within these codes and they can struggle with other key experimental features, such as reproducing observed very low gas saturations. This may limit their use as a general predictive tool for some aspects of the evolution but they are a necessary step towards building understanding of the important experimental phenomena. Thus, in the application of these approaches, calibration, constraints and parameterization of the codes emerge as key considerations in the modelling of advective gas, as well as the understanding of the key repeatable processes from gas flow experiments.

The models did provide a valuable service in aiding the interpretation of the experimental data and highlighted potential alternative interpretations of the experimental boundaries. Most importantly, the comparison of multiple approaches and simulation results clearly demonstrated that explicit representation of the injector is very important in order to produce a robust model, as the vast majority of the gas in the experimental system is held in the injector vessel and not in the clay sample itself.

## 2.6 Outstanding Issues

The work for this task has illustrated the complexity of advective processes in compacted clays, both in terms of the mathematical models adopted (and their limitations) and experimental interpretation. While some good results have been obtained, along with improved understanding there are a number of key questions that remain unanswered and will be the subject of future work:

- To what extent are the stochastic behaviors seen in the experiment important for 'real' scale applications? Do these complex behaviors that are not necessarily reproducible between experiments need to be represented explicitly or implicitly in the models?
- Given the ambiguity in interpretation of some of the experimental measurements, what are the key metrics we should be using to compare how 'good' the various approaches are?
- Many of the modelling approaches require very high resolution grids and long run-times. To what extent can these approaches be adapted to work efficiently at larger scales?
- The clays considered in this phase are relatively simple, in that anisotropy and heterogeneity is minimal. How can the approaches developed here be extended to more complex mineralogies and fabrics?

## 2.7 Future Work

Plans are in place for the next phase of DECOVALEX, to extend the work considered here to include field scale tests such as the Large-scale gas injection test (Lasgit). This highly instrumented test is based around a mock canister, encapsulated in bentonite/pellets, and placed within a deposition hole at the Äspö underground research laboratory (Sweden). The expansion of the numerical approaches to a full-scale test will provide an

invaluable tool to help to inform the modelling approaches and assess the impact of upscaling of gas flow on repository layout and therefore the design of any future facility.

# 3 Task B – Fault Slip Experiment

## 3.1 Background and Motivation

Within low permeability host rocks the heat generation associated with decay heat from radioactive waste can lead to substantial changes in pore-pressure due to differential expansion of the water and rock skeleton. Such changes in pore pressure may lead to mechanical damage of the host rock or may affect the stability of faults due to increased potential to reactivate such features. Such reactivation can lead to significant increases in the permeability of the faults, leading to a the risk of the low-permeability host rock being partially or completely bypassed, hence potentially reducing the degree of containment for the facility.

Task B addresses this area of potential concern by examining a series of fault activation experiments (FS experiment) recently performed at the Mont Terri underground research laboratory, Switzerland. The FS experiment explores the coupling between fault reactivation in a clay host rock and the potential for enhanced fluid displacement through a previously low-permeability formation. Based on this experiment, the DECOVALEX-2019 Task B addresses how the change in permeability induced by the fault activation and the resulting fluid flow within the fault can be simulated including the dependence on its mechanical behavior. This will support the understanding of the processes during fault activation itself and it can help to determine consequences for contaminant transport due to potentially created permeable flow paths in otherwise low permeability argillaceous rocks.

## 3.2 Organization and Participation

Task B was organized into three Steps. Step 1 was a benchmarking exercise looking at simplified systems analogous to the FS experiment. Step 2 considered data from the minor fault reactivation component of the FS experiment, while Step 3 considered a more complex fault reactivation of the main fault. The following organizations participated in the technical work for the task:

1. UFZ:Helmholtz Centre for Environmental Research, Germany;
2. BGR: Federal Institute for Geosciences and Natural Resources, Germany;
3. CNSC: Canadian Nuclear Safety Commission, Canada;
4. ENSI: Swiss Federal Nuclear Safety Inspectorate; Switzerland;
5. Department of Energy (DOE) supporting Lawrence Berkeley National Laboratory (LBNL) USA;
6. Korean Atomic Energy Research Institute (KAERI) supporting the Korea Institute of Geoscience and Mineral Resources (KIGAM), Republic of Korea;
7. SSM: Swedish Radiation Safety Authority (Strålsäkerhetsmyndigheten) supporting DynaFrax Germany; and
8. Taiwan Power Company, supporting INER(Institute of Nuclear Energy Research), Taiwan

Full details of the work performed can be found in Graupner et al. (2020).

## 3.3 Experimental Data

The Fault Slip (FS) experiment at the Mont Terri Underground Research Laboratory (URL) in Switzerland consisted of a series of controlled field stimulation tests conducted in spring and fall of 2015 in the Main Fault intersecting the clay formation at Mont Terri. The apparatus used for the injection tests is composed of surface equipment to conduct the test and acquire the data, and a downhole probe that allows simultaneous measurements of displacement, pore pressure and injection flow (Figure 8). Four interval tests were conducted beneath (test 47.2m), within (test 44.65m) and above (tests 40.6m and 37.2m) the Main Fault Core (FC) in borehole BFS2. Pressure and flow-rate time variations at the tests conducted outside the fault core (tests 37.2m, 40.6m and 47.2m) are characterized by an initial pressure increase without significant flow, followed by a sudden increase in the flowrate that occurs without any significant increase in pressure, indicating that the tested geological structure is able to readily accept fluid after the initial pressure increase.

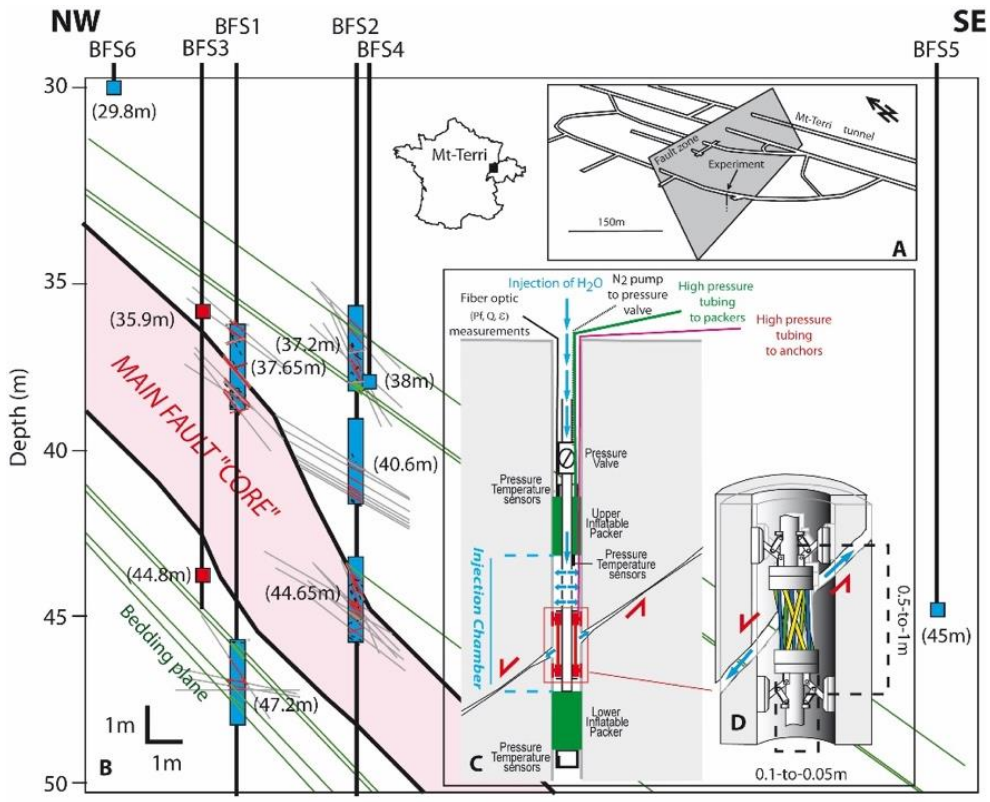


**Figure 8. (A) Three-dimensional view of the Mt Terri Main Fault plane with the location of the FS experiment; (B) Simplified cross section of the Main Fault with the blue rectangles indicating the location of the packed-off sections; (C) SIMFIP test equipment setup; (D) Schematic view of the three-dimensional deformation unit. Tubes are differently colored to show that they display different deformations when there is a relative movement of the rings anchored to the borehole wall across the activated fracture (Guglielmi et al., 2017).**

## 3.4 Task Approach and Selected Results

Information about the modelling approach, code etc for each team is given in Table 4. While there were a wide range of codes deployed, there were three broad approaches to representing the fault zone; 1) solid elements; 2) interface elements; and 3) a 'core fracture + damage zone' model within a particle flow code.

Step 1 involved a simplified representation of the fault plane and geometry and was intended for the modelling teams to familiarize themselves with the problem and allow for necessary model developments and testing related to modelling of fault activation processes (Figure 9). For Step 1, two different types of fracture hydromechanical behavior were defined: FM1 representing a case dominated by rupture propagation of an initially impermeable fracture, and FM2 representing re-opening of an initially permeable fracture. A set of additional benchmark tests were also defined because the

initial model comparison of the FM1 and FM2 benchmarks tests results showed significant deviations between the teams that, in many cases, were difficult to explain and seemed to be partially related to the modelling approach used. These additional benchmark simulations were defined based on the 3D FM2 case but specified with gradually increasing complexity to identify the points of divergence between teams' results. With the help of the simplified benchmark tests, it was possible to identify most of the differences in the modelling approaches, the initial and boundary conditions and the parameters between the teams. Based on these improvements, the results of the FM1 and FM2 steps show overall a good agreement between the teams, especially in the case of FM2. The extent and the stepwise change of relative anchor displacement is comparable between both cases of fault behavior, but evolution of pressure and displacements in the monitoring points as well as water flux is completely different for FM1 compared with FM2. In the case of FM1, significant amounts of water only flow into the fault during fault activation and thus pressure increase and displacement at the monitoring point starts when the rupture of the fault arrives there. In the case of FM2, a stepwise increase of pressure, displacement and water flux at the monitoring point with stepwise increasing injection pressure can be seen.

**Table 4. Overview about the model teams participating at the task.**

| Team | Computer Code | Fault representation | Funding Organization |
|---|---|---|---|
| **BGR/UFZ** | OpenGeoSys 6 | Interface | BGR |
| **CNSC** | COMSOL Multiphysics® | Solid elements | CNSC |
| **ENSI** | OpenGeoSys 5 | Solid elements | ENSI |
| **INER** | 3DEC | Interface | INER |
| **KIGAM** | TOUGH2-FLAC3D | Interface | KIGAM |
| **KIGAM** | | Solid elements | |
| **LBNL** | TOUGH2-FLAC3D | Solid elements | DOE |
| **LBNL** | 3DEC | Interface | |
| **DynaFrax*/SSM** | PFC2D & PFC3D | Core fracture + Damage zone | SSM |

* Joined DECOVALEX-2019 in the last project year.

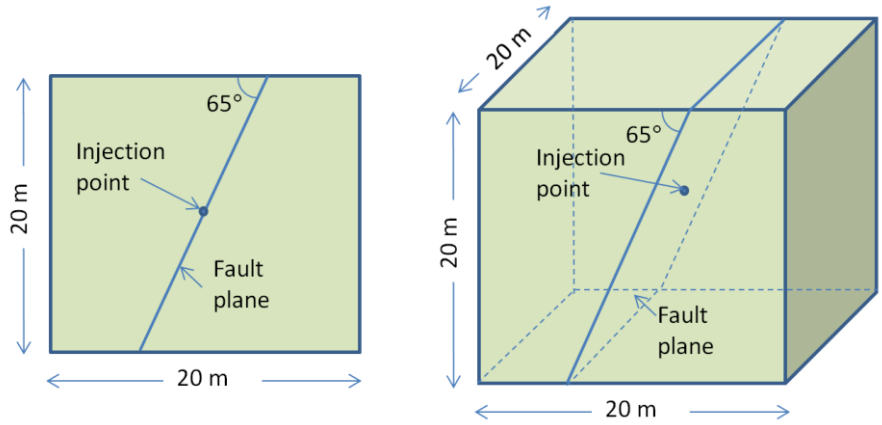


(a) (b)

**Figure 9. (a) 2D and (b) 3D model geometry for Step 1 benchmark calculation of injection induced fault activation.**

Step 2 considered the interpretative modeling of the observed response of the minor fault activation experiment (Figure 10). The results of the teams for Step 2 compare well to the measured initiation of the rupture, which took place after approximately 410 seconds of injection. The measured and simulated pressure increases very quickly, although the measured pressure peak appears to significantly fall and the measured drop of pressure after reducing the injection pressure to 3.4 MPa is slightly lower. The measured pressure and flow rate evolution suggests that the conceptual model of FM1 is more suitable to represent the fault behavior. The measured injection rate was well captured by the simulation results of the teams. Indeed, the induced permeability change with opening is a factor that affects the peak flow, including fracture-creation aperture and fracture-normal stiffness. Therefore, a second main output is that the description of the permeability changes based on the opening of the fault seems to be representative of the observed changes during the test.

Example results for Step 2 are shown in Figure 11. Points '2' and '3' are defined comparison points in the model domain. The results show that while the overall form of the results are very similar between the teams, there is substantial variation in magnitude of displacements and in the details of the transient behaviour for the fluid flow (as seen in the pore pressures at points '2' and '3').

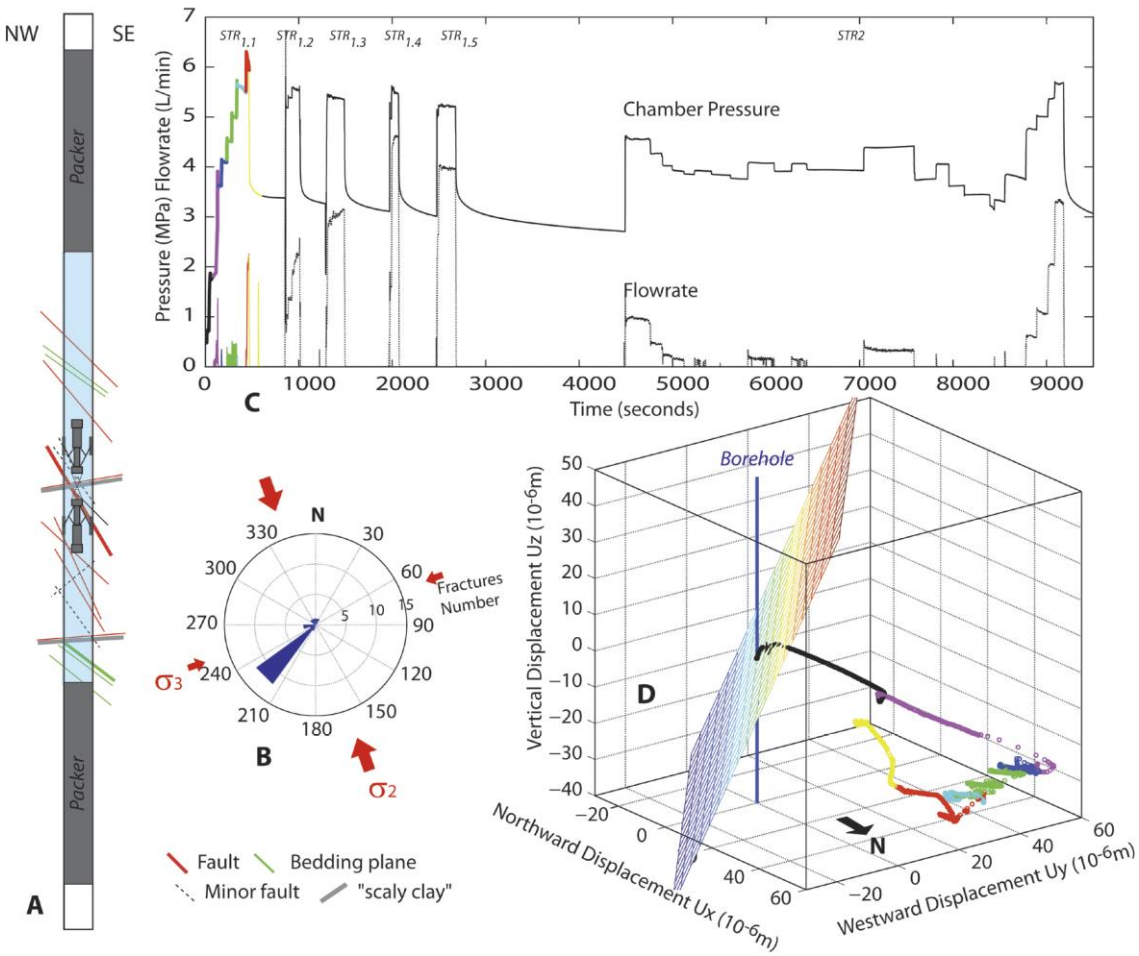


**Figure 10. A – Schematic structural view of the injection chamber with the location of the displacement instrument, B – Rose diagram of fractures and principal stresses orientation (after Martin and Lanyon, 2003), C – Chamber Pressure/Flowrate-vs-time variations; D – Three-dimensional view of the borehole displacements during STR1.1 cycle (plane figures the average fault strike and dip, colors refer to the different pressure steps figured in C).**

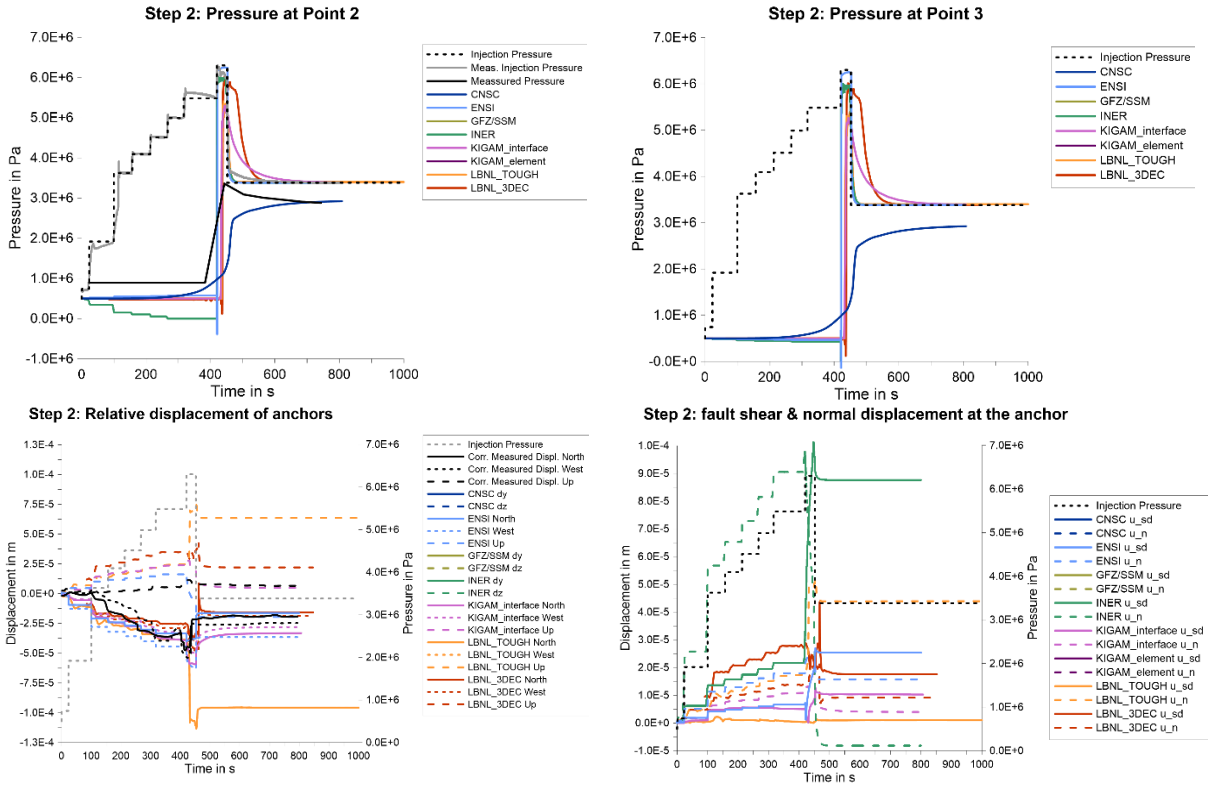


**Figure 11. Comparison of team results for Step 2 for pressures at two monitoring points, fault shear and fault-normal displacement, and relative displacements at the anchors**

Step 3 focused on another injection experiment conducted from another section of the same injection borehole, which resulted in shear activation and permeability changes along the main fault. Field data related to Step 3 were provided before the start of Step 3 modeling (as per Step 2). This case turned out to be much more complex to model as it requires the modeling of at least two intersecting discontinuities; one fracture connecting the injection well to the fault core and the interface between the fault core and the surrounding damage zone of the main fault. Therefore, only a few teams managed to provide simulation results. Those indicated again that the in situ fault behavior was similar to the conceptual model deployed in FM1, i.e. initial dominant fracture opening at the injection well along with rupture and propagation that later followed the interface between the fault core and surrounding host rock. However, different from Step 2, the modeling indicated a much larger magnitude of fault shear displacement that was triggered by sustaining a pressure above the fault opening pressure for a longer time period. Similar to the Step 2, the Step 3 data and modeling shows an apparent hydraulic closing of the fracture when the injection pressure was reduced below the fault opening pressure of approximately 4 MPa.

## 3.5 Key Outcomes

Overall, this DECOVALEX -2019 task has resulted in significant model developments and increased understanding of hydromechanical behavior of minor faults and fractures in low permeability shale. The modeling of the two different injection experiments to activate discontinuities within the Mont Terri Main Fault, including parts of the damage zone and close to the fault core, was done successfully after necessary model developments and adaptations. Faults were modeled successfully, either by interfaces or solid finite elements. The key for accurately modeling these experiments is a hydromechanical fault model that captures the abrupt activation behavior observed at the two activation experiments; in particular, an initial sudden increase in fracture permeability and flow rate along with a rupture opening and propagation that is triggered at a certain injection pressure magnitude higher than the estimated stress normal to the discontinuity, followed by a sudden hydraulic closure of the discontinuity that occurs when the injection fluid pressure is reduced to about 1 to 2 MPa less than the stress normal to the fault. This behavior was modeled by permeability enhancement resulting from damage induced permeability enhancement with plastic failure and a subsequent permeability reduction as a results of elastic fracture closure. In general, the fault hydromechanical behavior was captured best when modeling a propagating rupture along an existing weakness plane that caused some additional damage-enhanced permeability, simulated by a creation aperture or damage-enhancing factor on permeability. Such a model could capture the observed behavior of abrupt flow increase when pressure increases above the pressure required to propagate the rupture, and the subsequent flow decrease once the injection pressure was lowered below a threshold pressure to hydraulically close the fracture.

## 3.6 Outstanding Issues

The closure of fracture permeability is an important and beneficial feature for nuclear waste disposal in argillaceous clays, to provide a self-sealing mechanism to keep the host rock barrier tight. The models developed and tested within this DECOVALEX task can be applied to predict such behavior at a repository site in argillaceous claystone, but the hydromechanical fault activation models would ideally be tested and validated by site specific experiments of the type studied in this task.

The work here illustrated the different sensitivities of different numerical approaches when modelling such a system, and the different strategies required to get the best

results. Given these difficulties, predictive studies would appear to be a useful next step to build confidence in the robustness of the mathematical models being used.

## 3.7 Future Work

No specific plans for continuation of this project in DECOVALEX are in place, however new experiments at Mont Terri based on the highly-successful experiments used for Task B are ongoing, and may be used in a future DECOVALEX phase. These new experiments are focused on the long-term behavior of activated faults.

# 4 Task C – Groundwater REcovery Experiment in Tunnel (GREET)

## 4.1 Background and Motivation

The construction of underground facilities for the geological disposal of radioactive waste will change the environmental conditions present before construction, potentially quite significantly. These initial conditions will be characterized using surface-based investigations before the construction of the facility. However, it is still unclear whether the disturbed environment will fully recover after the facility is closed and resaturates, bearing in mind the presence of long-term transients present at potential facility locations.

Task C aims to develop modelling and prediction methods using numerical simulations based on a large scale Closure Test Drift (CTD) at the Mizunami Underground Research Laboratory (Figure 12). This experiment is designed to examine the post-drift-closure environment recovery processes and includes an artificial filling process to accelerate the timescales of the experiment.

The primary features of interest were the water pressure drawdown and recovery, and the variation of water chemistry during the tunnel excavation and closure, as observed in the monitoring boreholes and the CTD itself. Full details are available in Iwatsuki (2020).

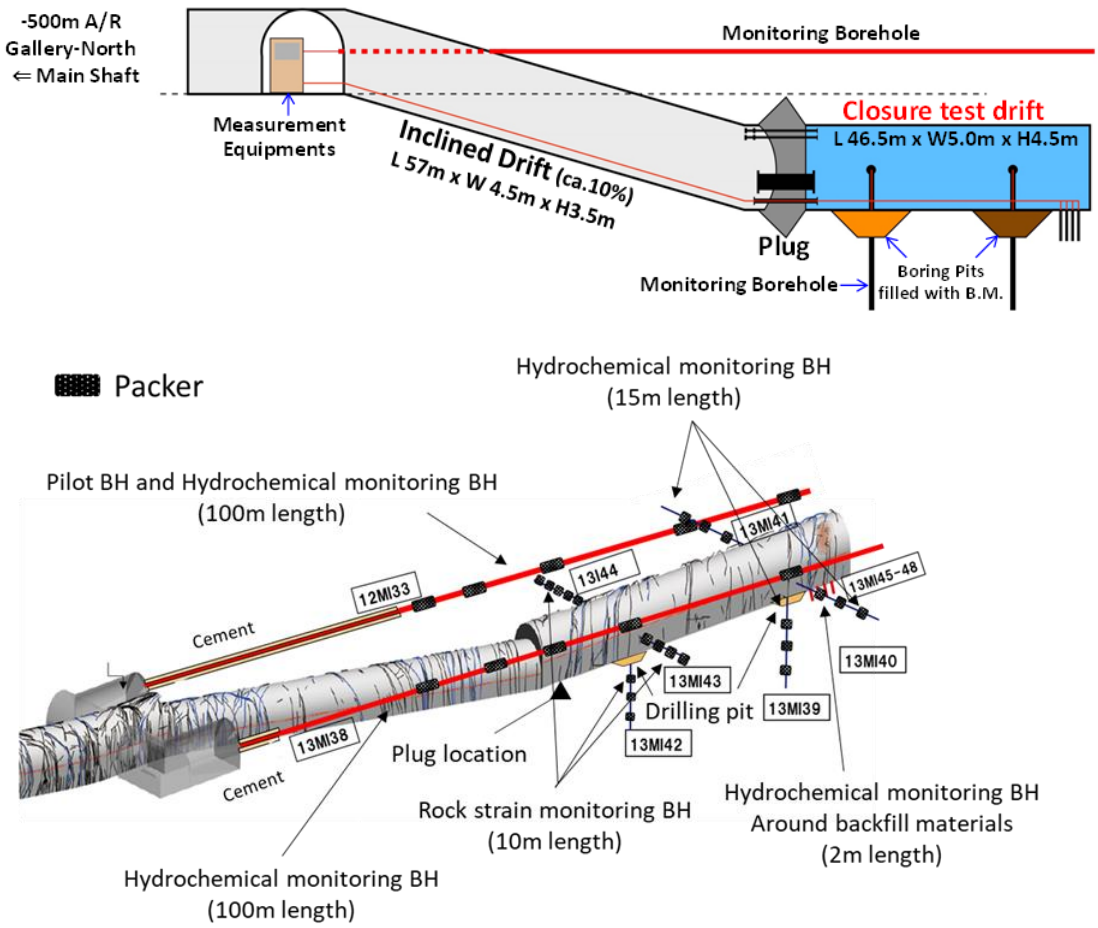


**Figure 12. Experimental facilities around the CTD for GREET.**

## 4.2 Organization and Participation

Three research teams, JAEA, Sandia National Laboratories in the United States (SNL), and the Technical University of Liberec in the Czech Republic (TUL) were challenged to simulate the observed environmental changes. The Task consisted of following three main steps.

- Step1: Modelling and prediction of environmental disturbance by CTD excavation
- Step2: Modelling and prediction of environmental recovery by CTD isolation
- Step3: Modelling and prediction of the long-term environmental condition after CTD isolation

## 4.3 Experimental Data

The GREET (Groundwater REcovery Experiment in Tunnel) project was conducted at the Mizunami Underground Research Laboratory of the Japan Atomic Energy Agency (JAEA) to evaluate the environmental recovery process around research galleries in fractured crystalline rock. The experiment has been planned to observe any environmental changes following the refilling of the Closure Test Drift (CTD) with water. The baseline hydro-mechanical-chemical (H-M-C) condition was identified before the excavation of the CTD. Then excavation of the CTD and isolation by a water-tight plug, and subsequent flooding with groundwater was conducted (Figure 13). Environmental disturbance and recovery were observed for more than 6 years. In the experiment, hydraulic and chemical changes of groundwater were obviously dependent on the fracture distribution in the granite. During the tunnel closure experiment, the water pressure in the intact rock mass zone showed less of a response, while that in the fractures connected to the CTD directly reflected the change of the water pressure in the CTD. These observations indicated that the rock mass around the CTD has a high heterogeneity. Cl concentrations in the fractures varied through different mixing with groundwater derived from shallow or deep depths. The groundwater in the CTD evolved to alkaline and reducing conditions.

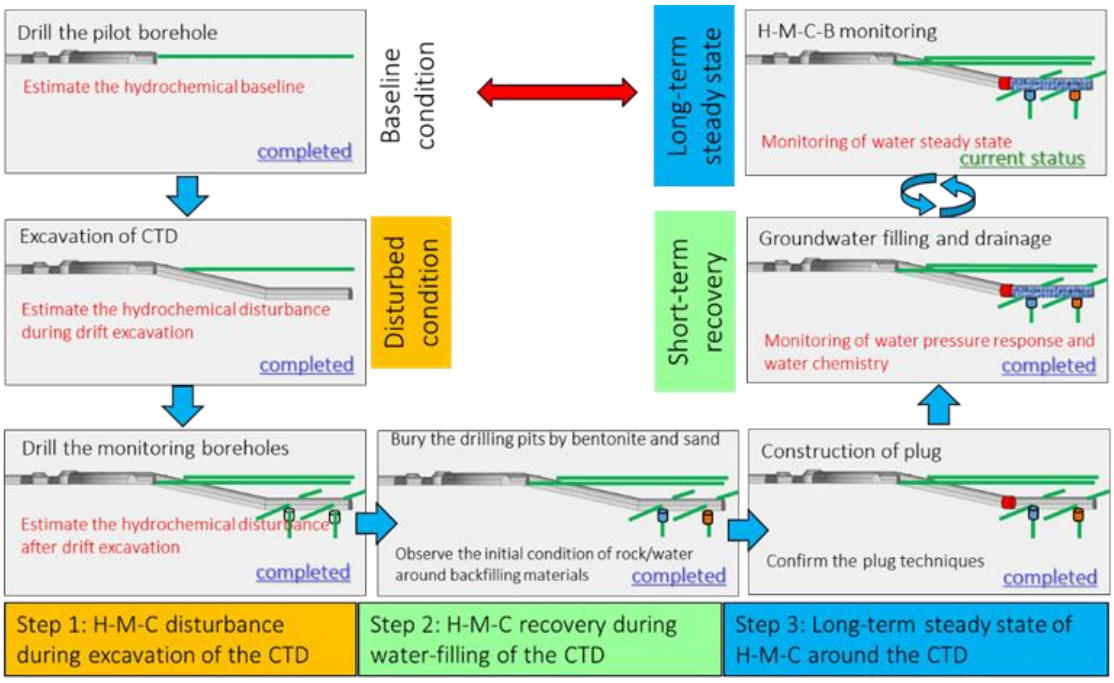


**Figure 13. Outline programme for Task C.**

## 4.4 Task Approach and Selected Results

As to modeling approaches, a stochastic model using a discrete fracture network (DFN) capability, an equivalent continuum porous media (ECPM) model, and deterministic approach based on mixed-hybrid finite element methods were applied by the JAEA, SNL and TUL teams respectively (Table 5, e.g. Figure 14). Furthermore, reactive transport modelling and basic thermodynamic analyses were examined to capture the chemical evolution of isolated groundwater in the CTD. The JAEA team constructed a reference model to check the viability of the original simulation code 'COUPLYS', and then examined the sensitivity of the various parameters to the simulation results. The target parameters were estimated by using a DFN model with 100 realizations based on the fracture data (size distributions, orientation, volumetric intensity, the relationship between the aperture and permeability and the radius) and the ECPM model created from the most representative DFN model. SNL also developed a DFN model with 10 realizations and ECPM models converted from each DFN model. The simulations were conducted using the coupled 'DAKOTA-PFLOTRAN' codes. The TUL team applied a deterministic approach based on a multi-dimensional concept (discrete fractures + equivalent continuum) using the code 'Flow123d'.

**Table 5. Codes, methodologies and funding Organizations for Task C.**

| Team | Computer Code | Methodology | Funding Organization |
|---|---|---|---|
| **JAEA** | COUPLYS | Stochastic, DFN-ECPM | JAEA |
| **SNL** | DAKOTA-PLFLOTRAN | Stochastic, DFN-ECPM | DOE |
| **TUL** | Flow123d | Deterministic – equivalent continuum + discrete features | SURAO |

Example results showing comparison of pressures in the CTD post-flooding, pressures in the monitoring borehole and example calculated chloride concentrations are shown in Figure 15 to Figure 17. The CTD pressure drop, with consequent impact on the monitoring points, is related to a leak around the CTD isolation plug and was the cause of significant calibration effort. The Cl concentrations shown calculated by JAEA were the produce of considerable manual calibration and required effectively connecting different parts of the CTD to different heights in the wider geology (there is a significant chloride concentration gradient at the Mizunami URL, with higher concentrations at depth) in addition to the localised heterogeneity created through the DFN/ECPM approach.

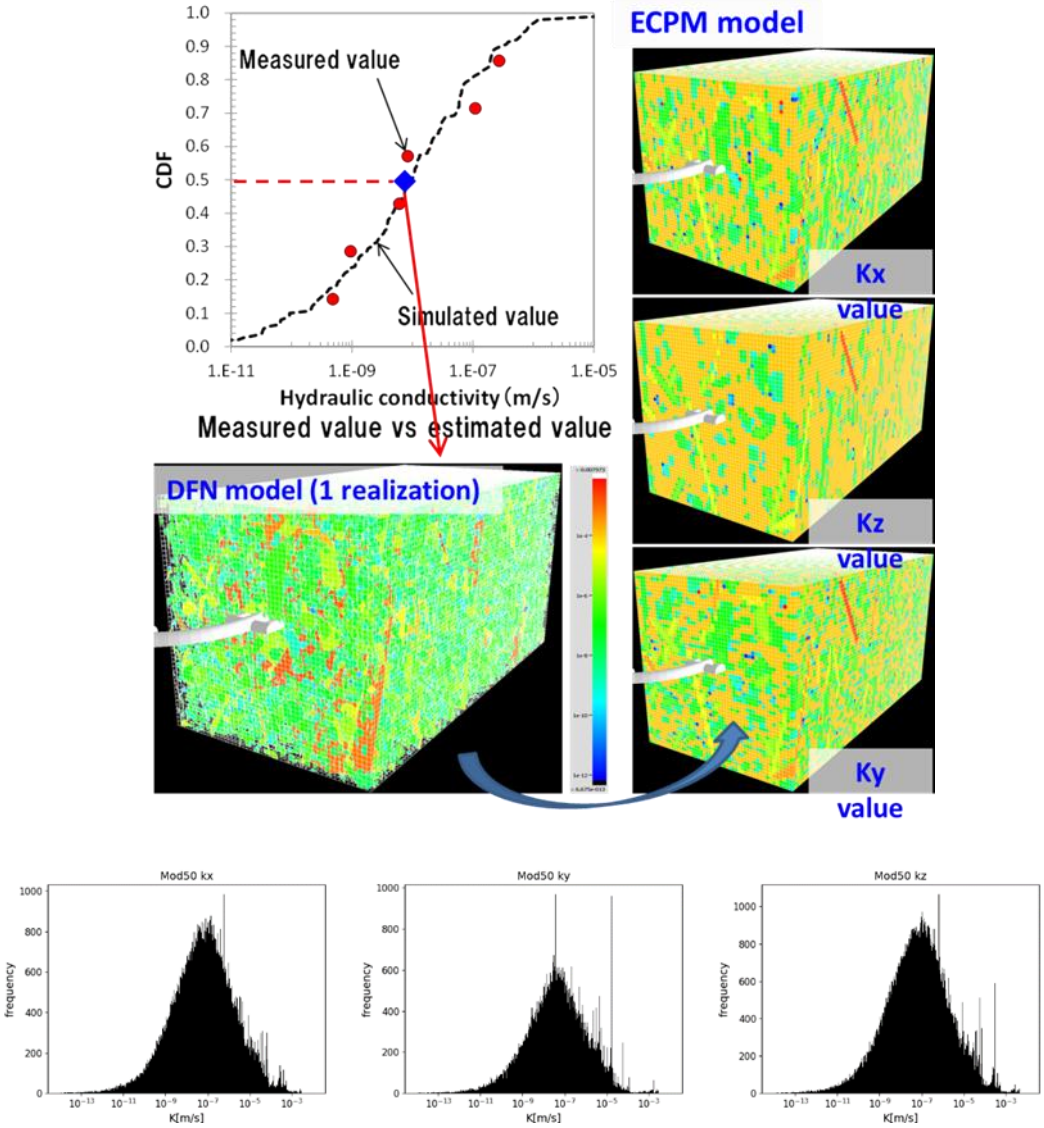


**Figure 14. DFN model for ECPM modelling from the JAEA approach. Spatial distribution of anisotropic hydraulic conductivity (upper right) and its frequency (lower)**

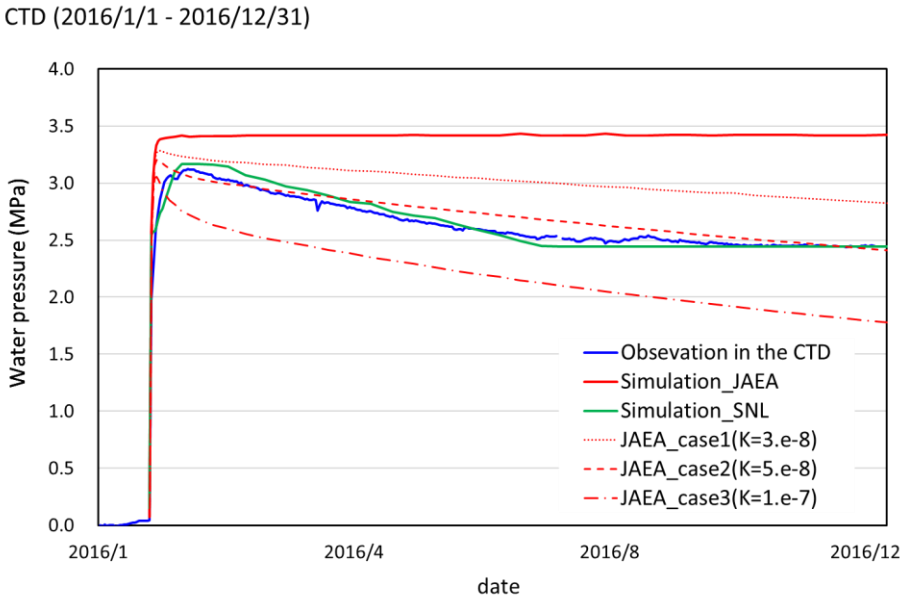


**Figure 15. Simulated water pressure changes in the CTD.**

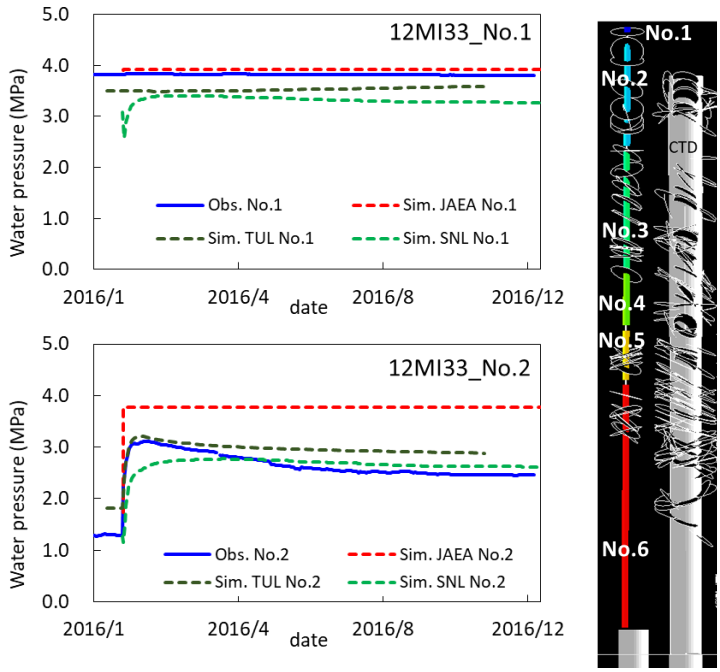


**Figure 16. Simulated water pressure changes around the CTD and monitoring points 1 and 2.**

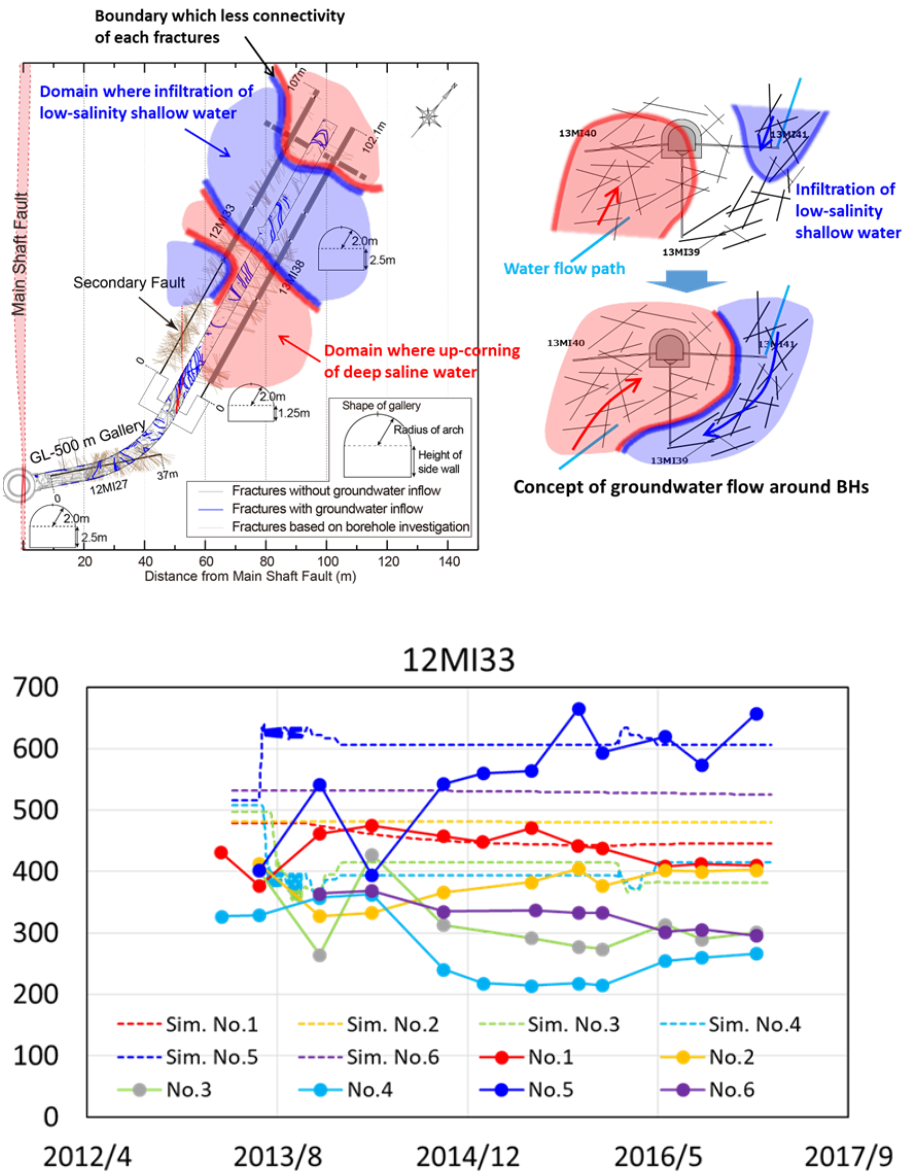


**Figure 17. Top: conceptual model adopted by JAEA to represent the observed chloride concentrations at the CTD. Bottom: simulated Cl concentration (mg/l) by measurement date in the12MI33 borehole as calculated by the JAEA team.**

## 4.5 Key Outcomes

The combination of a stochastic and deterministic approach with an iterative calibration considering high permeability fractures was seen to be successful in representing the range of groundwater inflow rates into the tunnel, hydraulic drawdown and the recovery. Using the ECPM models converted from the DFN models, with a deterministic approach and inverse modelling, the variation of Cl concentration in each monitoring point around the tunnel could not be reproduced while retaining the observed hydraulic

characteristics. This suggests the importance of modelling the channelization or larger-scale heterogeneity within the water-conducting fractures in the fracture network and some success was had in representing such features manually. Currently, it is possible to represent the general range of Cl concentration variation using the current modelling methodology, but not the specific details. It is expected that the developed modelling and simulation methods in Task C can be applied to all phases of a HLW geological disposal project in fractured rock.

## 4.6 Outstanding Issues

When considering the isolated groundwater evolution, thermodynamic analysis can identify dominant water-mineral interactions that affect the future chemistry of isolated groundwater in the tunnel. Reactive transport modelling including these minerals has not yet been completed, but the spread of alkaline groundwater from CTD to rock was inferred to be retained in the vicinity of the shotcrete. Further checks of the applicability of the reactive transport modelling methodology is required to estimate the long-term advection or diffusion of chemically distinct water around the tunnel in the future.

Furthermore, it is clear that it is difficult to be predictive regarding transport calculations especially, and should robust predictions be required from an operational or post-closure safety perspective, there remains a considerable amount of work to be performed.

# 5 Task D – Hydro-Mechanical Interactions in Bentonite Engineered Barriers (INBEB)

## 5.1 Background and Motivation

Many radioactive waste disposal concepts use compacted bentonite to act as a key part of the engineered barrier system. While the precise safety functions vary according to concept, using compacted bentonite requires a certain bentonite density such that the required hydro-mechanical properties are achieved post-closure. The presence of significant heterogeneity in the bentonite barrier could lead to the barrier not performing as expected, hence understanding how heterogeneities in emplaced bentonite might occur and how they may or may not homogenize with time is of high interest for such disposal concepts.

Task D of the DECOVALEX-2019 project is therefore devoted to the study of the hydro-mechanical (HM) and thermo-hydro-mechanical (THM) Interactions in Bentonite Engineered Barriers (INBEB). Special attention is paid to the evolution of barrier heterogeneity under transient conditions. A proper understanding of the processes occurring during the transient period requires the appropriate simulation of the behavior of the engineered barrier by means of coupled numerical analyses. In this context, the main objective of the Task is to assess the capabilities of numerical formulations and codes to simulate and interpret the HM and THM behavior of the bentonite barrier, with a particular focus on the final state reached on saturation.

Full details on the work can be found in Gens (2020).

## 5.2 Experimental Data

The Task is structured around two large scale in situ experiments that were subjected to well-managed dismantling operations that provided direct observations of the state of the barrier after long test periods. The experiments encompass a range of barrier configurations and test conditions.

The EB experiment (Figure 18) was carried out in the Mont Terri underground laboratory. The barrier is mostly made up of granular bentonite with some bentonite blocks to provide support for a dummy canister. It is an isothermal test with artificial hydration. Dismantling took place at the end of the 10.7 years testing period.

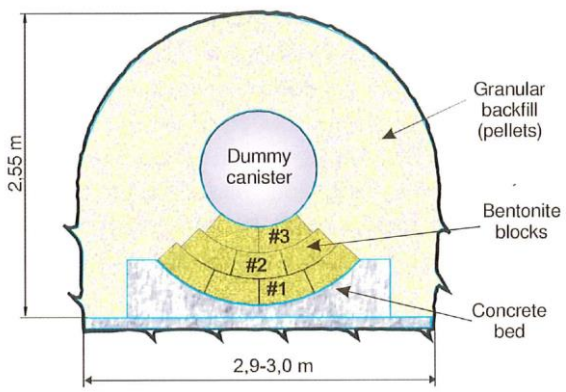


**Figure 18. EB experimental layout (Mayor et al., 2007)**

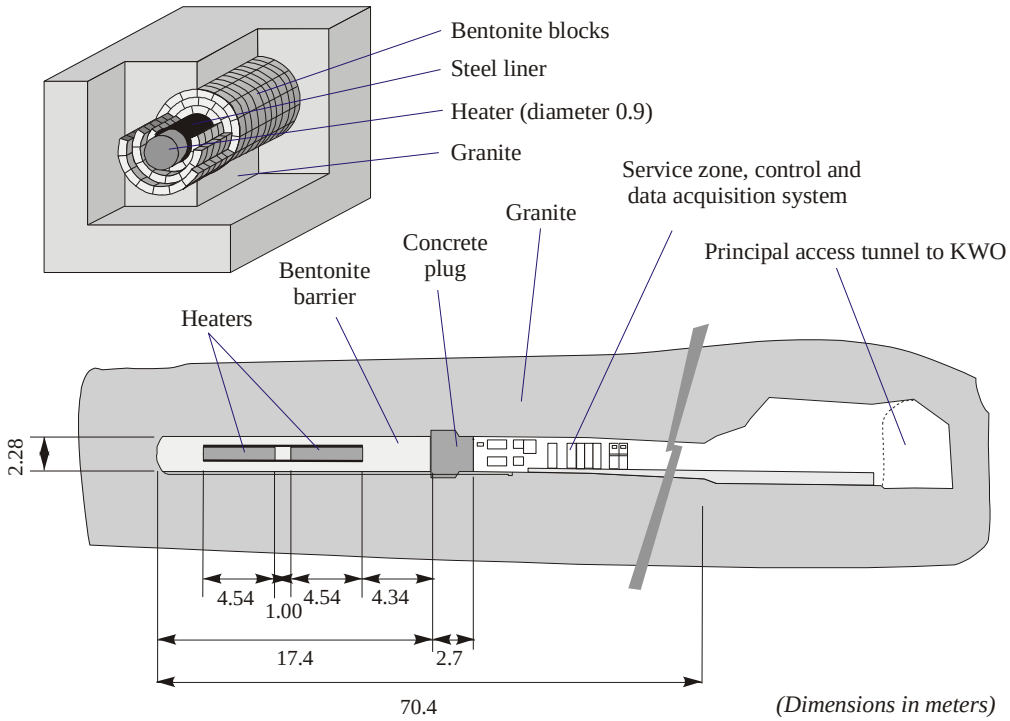


**Figure 19. FEBEX test layout (ENRESA, 2000)**

The FEBEX test (Figure 19) was performed at the Grimsel Test Site. The barrier is composed of bentonite blocks only. It is a temperature-controlled non-isothermal test combined with natural hydration from the rock. There were two dismantling operations, a partial one after 5 years of heating and a final one after a total of 18.4 years of heating.

The monitoring of the EB test showed a progressive hydration and the development of swelling stresses. The barrier was found to be saturated at the end of the test. Dismantling data revealed that there had been a nearly complete homogenization between blocks and pellets in spite of their very different initial dry densities. The FEBEX experiment also exhibited the progressive hydration of the barrier and the associated development of swelling stresses. In the initial phases of the test, the bentonite close to the heater dried and vapor transport affected the local variations of relative humidity. In the first dismantling, the barrier was still far from saturation except close to the rock. The dry density had increased near the heater and had reduced in the vicinity of the rock, while keeping the average approximately constant. At the end of the test, the barrier was largely saturated but the dry density distribution was heterogeneous and practically unchanged from the first dismantling.

## 5.3 Participation and Organization

Four teams carried out the modelling of the two experiments: Institute of Geonics, of the Czech Academy of Sciences (IGN), supported by SÚRAO, Czech Republic, Japan Atomic Energy Agency (JAEA), Korea Atomic Energy Research Institute (KAERI) and National Central University of Taiwan (NCU), supported by Taipower.

The Task was organized in four successive main stages:

- Stage 1: Operational period of the EB experiment. Modelling of the EB experiment during hydration (10.7 years). The results of the analyses are compared with the data from the monitoring system.
- Stage 2: Post-dismantling period of the EB experiment. Computation/ prediction of the final state of the barrier is assessed against the data from dismantling.
- Stage 3: Modelling of the FEBEX "in-situ" test during the first 5 years of heating up to and including the first dismantling. The results of the analyses are checked against instrumentation data and the observations obtained in the partial first dismantling.
- Stage 4: Modelling of the FEBEX "in-situ" test after the first dismantling until the end of the experiment including the final dismantling. Modelling results are compared with instrumentation data and final dismantling observations.

## 5.4 Task Approach and Selected Results

A range of computer codes have been employed: COMSOL (IGN), THAMES and DACSAR 2D (JAEA), TOUGH2-MP/FLAC 3D (KAERI) and HYDROGEOCHEM 4.3/5.3 (NCU) – see Table 6. Except in two cases, 2D domain geometries have been used, plane strain for the EB test and axisymmetric for the FEBEX test (example pseudo 2D mesh shown in Figure 20). The use of 3D geometries did not lead to an improvement in results commensurate with the much larger computer resources required.

**Table 6. Codes, methodologies and funding Organizations for Task D at the end of the task.**

| Team | Computer Code | Basic Formulation | Mechanical Formulation | Funding Organization |
|---|---|---|---|---|
| **IGN** | COMSOL Multiphysics® | Richards' equation + vapour + mechanics | Non-linear elastic + swelling term | SÚRAO |
| **JAEA** | THAMES and DACSAR 2D | Unsaturated flow + mechanics | Unsaturated elasto-plastic model | JAEA |
| **KAERI** | TOUGH2-MP / FLAC 3D | Unsaturated flow + mechanics | BBM (Unsaturated elasto-plastic model) | KAERI |
| **NCU** | HYDROGEOCHEM 4.3/5.3 | Unsaturated flow + mechanics | Linear elasticity + swelling term | Taipower |

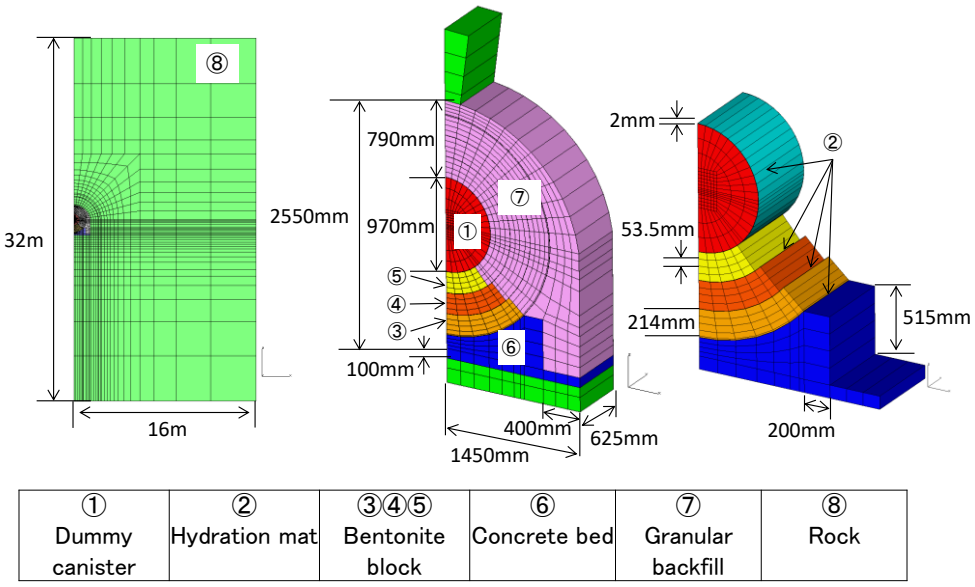


**Figure 20. Domain of analysis and finite element mesh used by JAEA for the EB test.**

All the analyses performed have been based on coupled TH and THM formulations. They involve the solution of the equations of water balance and liquid flow, equilibrium and, for non-isothermal problems, energy (heat) balance. One team (KAERI) also incorporated the air balance and gas flow equations. Although the final state of the barrier is likely to depend on the mechanical constitutive model, no new laws have been developed in the Task. No special models for pellets-based materials were formulated.

Example results are shown for EB and FEBEX in Figure 21 and Figure 22. While the results appear good for the bulk of the granular bentonite in the EB (representative section shown in Figure 21), it should be noted that the models could not reproduce the very low observed densities in the corner of the sections (RS6 or 8) – this very likely reflects initial heterogeneity, but a weakness in the models cannot be completely ruled out. Similarly, the teams struggled to reproduce the apparent vertical homogenization as evidenced by the canister displacements. For FEBEX, where the thermal gradient drives much of the variation, the teams were able to obtain a generally good match to the water content and dry density variation associated with the heaters (Figure 22), although in the case of the NCU formulation, the lack of vapor transport affects and the assumption of invariant of dry density affects the predictions of the bentonite behavior especially close to the heater.

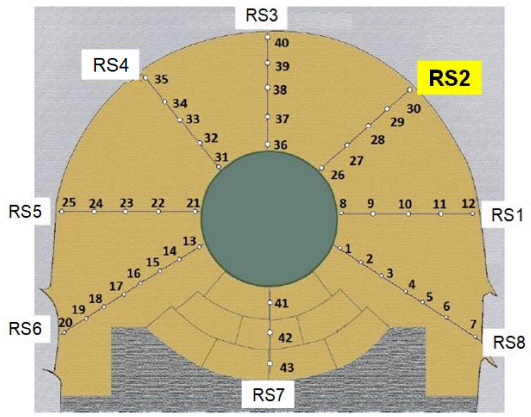


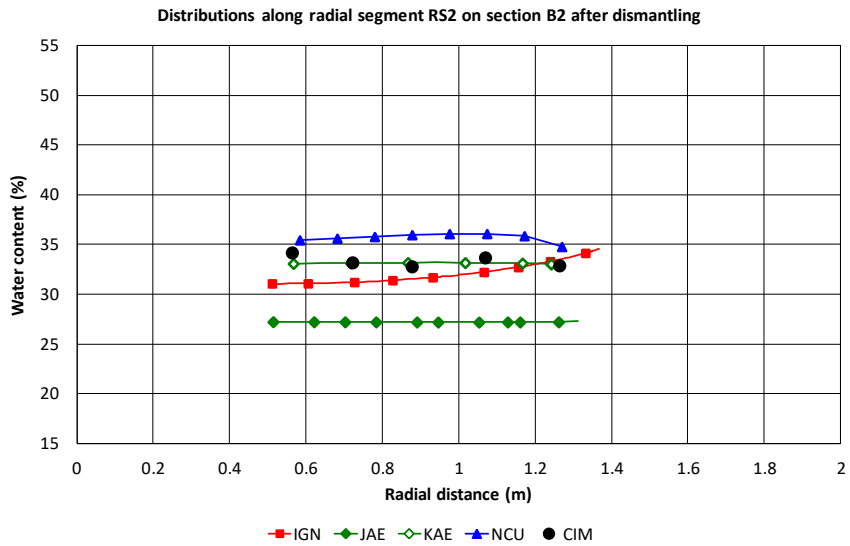


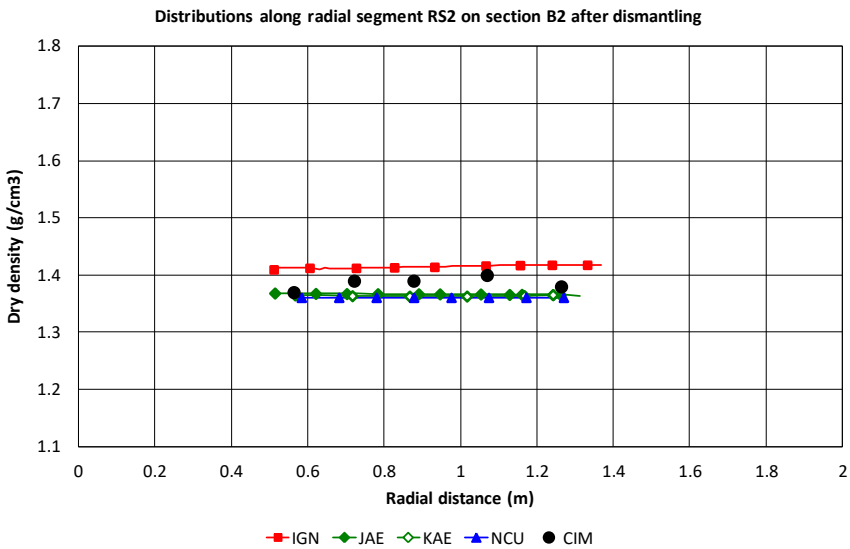


**Figure 21. Mass water content (top) and dry density (bottom) for EB. Modelling results vs. observations (CIM). Section B2, radii RS2 (granular bentonite). Initial mass water content: 4.2%, initial dry density: 1.36 g/cm$^3$.**

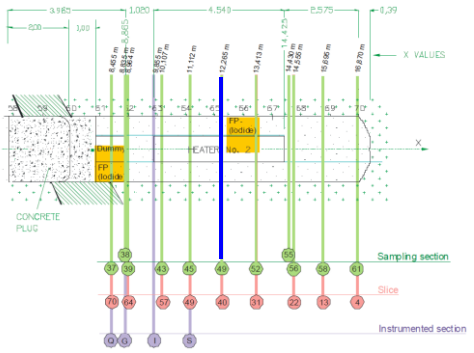


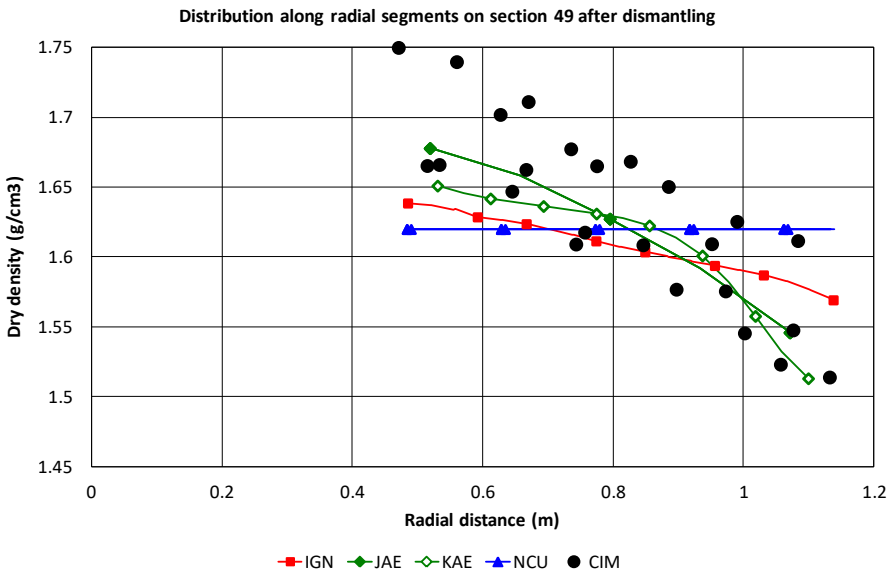


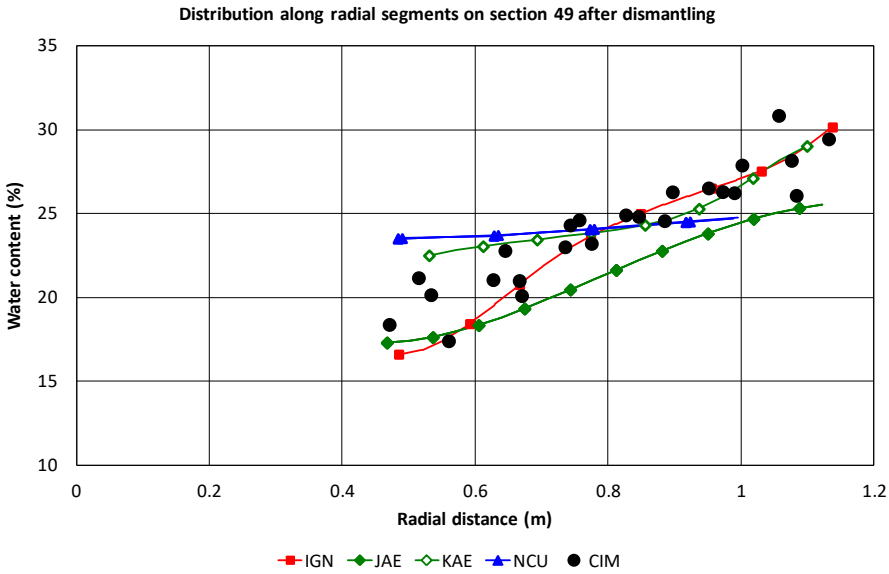


**Figure 22. Modelling results vs. observations (CIM) for FEBEX. Distributions of dry density (top) and mass water content (bottom) after final dismantling. Section 49.**

## 5.5 Key Outcomes

In general, the numerical models were able to represent adequately the global TH and THM behavior of the experiments modelled. The most important phenomena and their couplings appear to be incorporated in an appropriate manner. However, shortcomings were identified in some of the formulations that affected the capability of the models to simulate more closely the observed test behavior. The main ones were: neglecting the variation of hydraulic conductivity with porosity, the non-inclusion of vapor transport and the failure to incorporate the dependency of dry density on suction and stresses.

The vertical homogenization observed in the EB test was not generally reproduced by the numerical analyses. The evolution of the barrier in the FEBEX test was well captured by some but not all the models. It is likely that more advanced constitutive models for bentonite blocks and, especially, bentonite pellets may be required for a closer representation of their behavior, specially the mechanical one.

## 5.6 Outstanding Issues

It should be noted that the Task did not include any modelling involving blind predictions; the experimental results were available to the teams from the start. Therefore, the results presented here do not provide conclusive information on the predictive capabilities of the models. It is also important to realize that an adequate reproduction of one-off large scale in situ tests does not necessarily imply that all individual phenomena and processes are well represented in the modelling. To identify the effects and significance of individual processes, it is necessary to complement the large in-situ experiments with well-designed and closely controlled tests performed in the laboratory.

On the other hand, it is not immediately clear that representing all features and processes observed at the laboratory scale are required for large-scale applications, depending on the characteristics of the experiment and the predictions that are required. The work here has shown that, at the larger scale, different approaches can yield results that represent some aspects of the experiments better than others and hence the choice of methodology will depend, to some extent, on the modelling outcomes required.

# 6 Task E – Upscaling of Modelling Results from One-to-one to Field Scale

## 6.1 Background and Motivation

The Thermo-Hydro-Mechanical (THM) behavior of the Callovo-Oxfordian claystone (COx) is of great importance for the design and safety assessment of a high-level and intermediate-level long-lived waste repository. In particular, the overpressure generated by heat produced from high level waste is of interest. The excess pore pressure generated (caused by the water expanding faster than the rock matrix) has the potential for the COx to enter tension in the vertical direction, with the consequent risk of fracturing. Such fractures could reduce the effectiveness of the COx as a diffusive barrier to radionuclide transport and bypass engineered barriers in the repository design. This is why the design of the high level waste repository is such that this process cannot take place (i.e. no tensile stress). Therefore to be able to predict the hydraulic and mechanical condition of the host rock under thermal load is key to building confidence in the performance of a future radioactive waste disposal facility.

The purpose of Task E of the DECOVALEX-2019 project was to investigate upscaling approaches for THM modelling from small-scale experiments (some cubic meters) to full-scale experiments (some ten cubic meters) and finally to the scale of the waste repository (cubic kilometers). To achieve this aim, the data of two in-situ heating experiments performed by Andra (the French National Radioactive Waste Management Agency) in the Meuse/Haute-Marne Underground Research Laboratory (MHM URL) formed the basis for understanding the THM behavior of the COx at different spatial scales. The first experiment provided the reference values of the THM parameters by means of a calibration exercise and these were then used for a blind prediction and an interpretative analysis of the second experiment. The results of this work were then used at the whole repository scale to better understand upscaled effects of multiple disposals and key sensitivities and uncertainties at that scale.

For full details of the work conducted please see Plua et al. (2020).

## 6.2 Organization and Participation

The task was divided into the following main stages:

- Step 1: Benchmarking and code verification
- Step 2: Interpretive modelling of the TED experiment
- Step 3: Predictive modelling of the ALC experiment, followed by interpretive analysis and recalibration (as required)
- Step 4: 'Whole repository' analysis based on Steps 1-3.

Technical participation consisted of five research teams:

- Andra (France)
- Lawrence Berkeley National Laboratory (USA)
- NWMO (Canada)
- Quintessa (UK)
- UFZ/BGR (Germany)

In addition, a PhD student from Lille University, financed by DECOVALEX, joined on April 2018 to work on Step 3.

## 6.3 Experimental Data

The task used two main sources of experimental data, both at field scale, supported by a large quantity of laboratory data and field observations from the MHM URL.

The first experiment was the TED experiment, which used three small-scale heaters installed in boreholes constructed from the side of an access gallery, supported by an array of measurement points (temperature and pore-pressure) - Figure 23. Three 4 m long heaters which were installed at the end of 160 mm diameter and 16 m long boreholes in order to avoid the influence of the temperature variations of the GED drift

The second was a larger scale experiment, the ALC, which used a full-sized disposal borehole with dummy waste heat sources. The heated part of the ALC borehole is located in the main body part between 10 and 25 m deep and is made up of five heating elements. Each element is 3 m long and has a diameter of 508 mm. Instrumentation boreholes are drilled both from the GAN drift and the NRD niche, which is excavated itself from GRD drift - Figure 24. A mixture of temperature and pressure sensors were installed in single boreholes and multi-packer arrays. One borehole was also instrumented with strain gauges, but these strain data appeared not to be reliable; thus they were not used for the comparison.

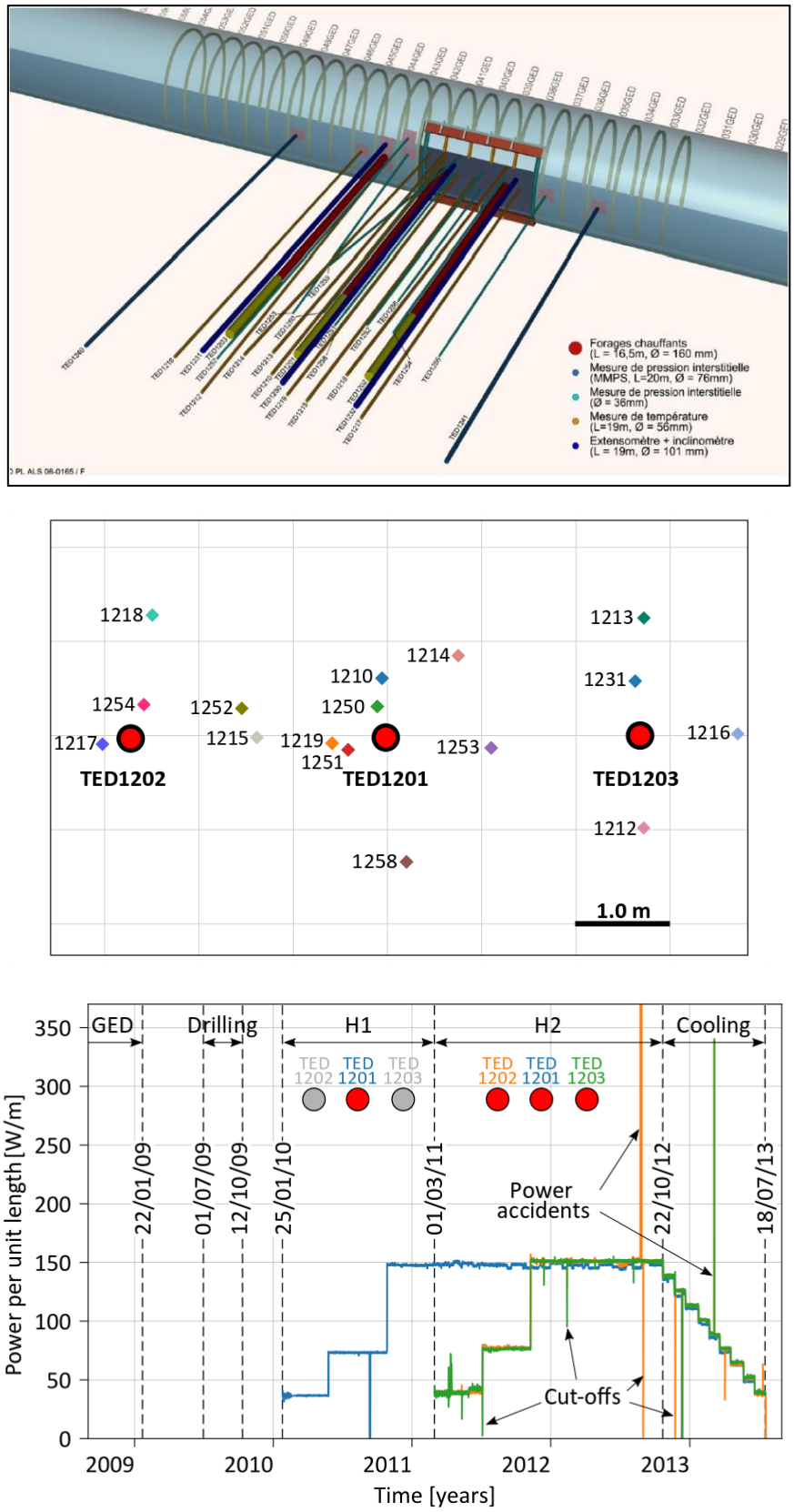


**Figure 23. Three-dimensional layout of the TED experiment (top) and location of different sensors of the TED experiment on the plane y = 14 m (middle), experiment timeline (bottom).**

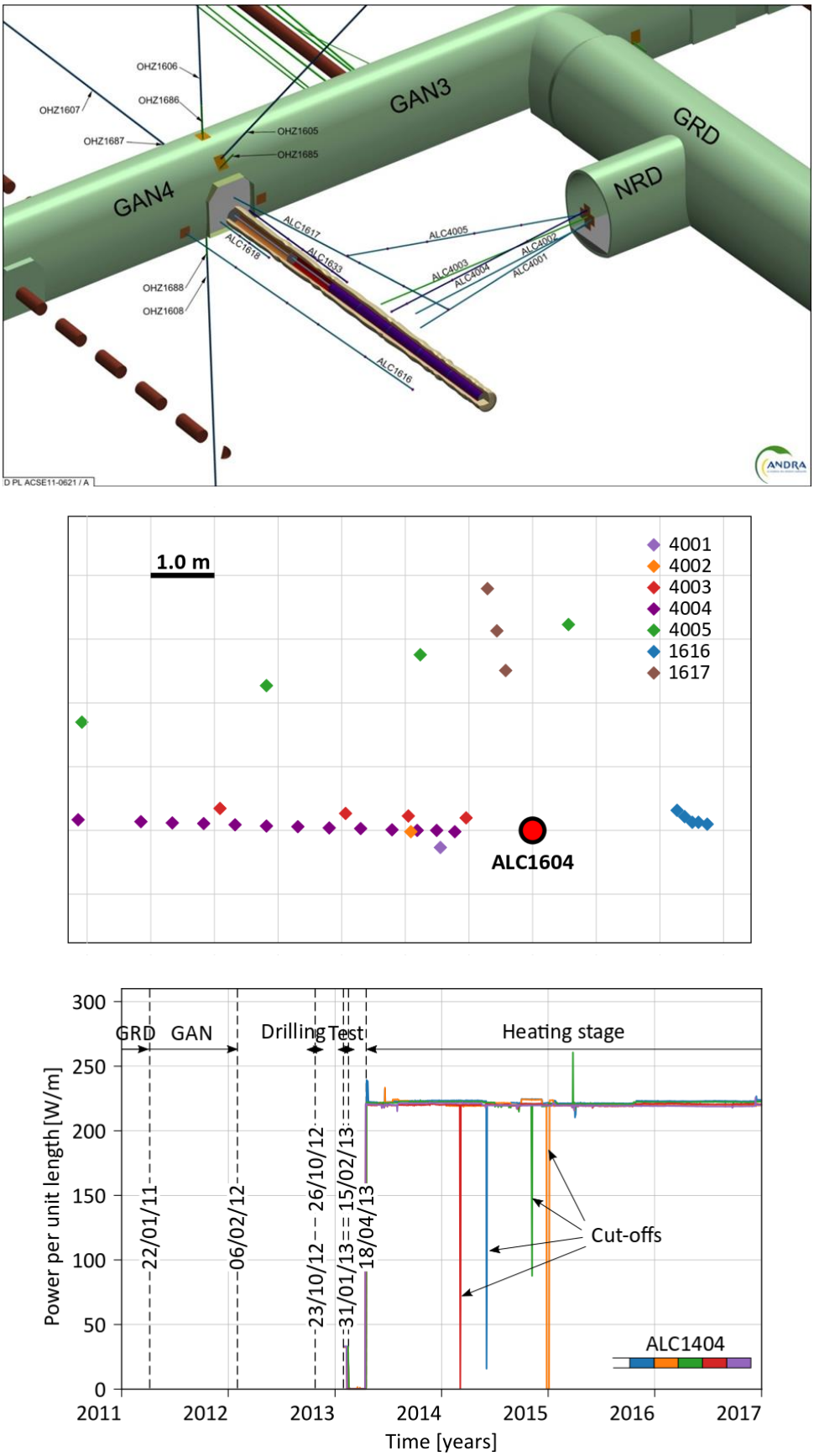


**Figure 24. General overview of the ALC experiment (top), YZ-view of the ALC experiment (middle), experiment timeline (bottom).**

## 6.4 Task Approach and Selected Results

All teams used the same basic poro-elastic methodology, combining thermal diffusion, Darcy flow (single phase – desaturation of the COx was judged negligible) and elasticity. Pore pressures were linked with stresses via effective stress theory and using Biot coefficients (see Plua et al., 2020). Some mechanical plasticity was examined in the context of gallery and borehole engineered damage zone (EDZ) formation and properties, but the teams all took different approaches in this regard. Therefore the main differences between the results of the teams relate to different parameterisation and modelling choices rather than fundamentally different mathematical models.

**Table 7. Modelling teams and numerical codes.**

| Team Acronym | Team | Code(s) | Funding Organization |
|---|---|---|---|
| Andra | French National Radioactive Waste Management Agency | COMSOL Multiphysics® and Code_Aster | Andra |
| LBNL | Lawrence Berkeley National Laboratory | TOUGH-FLAC | DOE |
| NWMO | Nuclear Waste Management Organization | COMSOL Multiphysics® | NWMO |
| Quintessa | Quintessa | COMSOL Multiphysics® and QPAC | RWM |
| UFZ/BGR | Federal Institute for Geosciences and Natural Resources and Helmholtz Centre for Environmental Research | OpenGeoSys | UFZ/BGR |

The benchmarking from Step 1 showed that details of the formulations, such as the equation of state for water density as a function of pressure and temperature and water viscosity, could lead to non-trivial differences in the results obtained, but otherwise the codes could give all give functionally identical results.

For the TED experiment, teams were able to obtain very similar results using similar thermal parameterisation and were able to fit the data well (Figure 25). However, all teams required a slightly lower heater power for the expected COx thermal properties to obtain the observed temperatures. This was felt likely to be the result of electrical

losses in the system, therefore, all the modelling teams agreed to use a correction coefficient of 95% to account for the power loss within the heaters moving forward. More variability was seen in the pressure response, mainly due to differing treatment of gallery construction and damage to the COx, but the overall parameterization and pressure response was consistent (Figure 26).

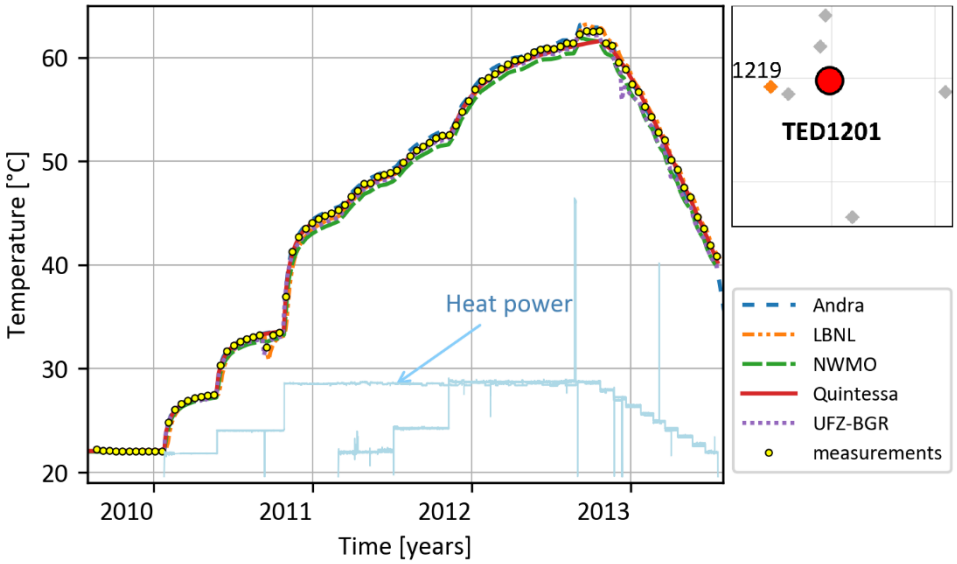


**Figure 25 Temperature evolution at sensor TED1219**

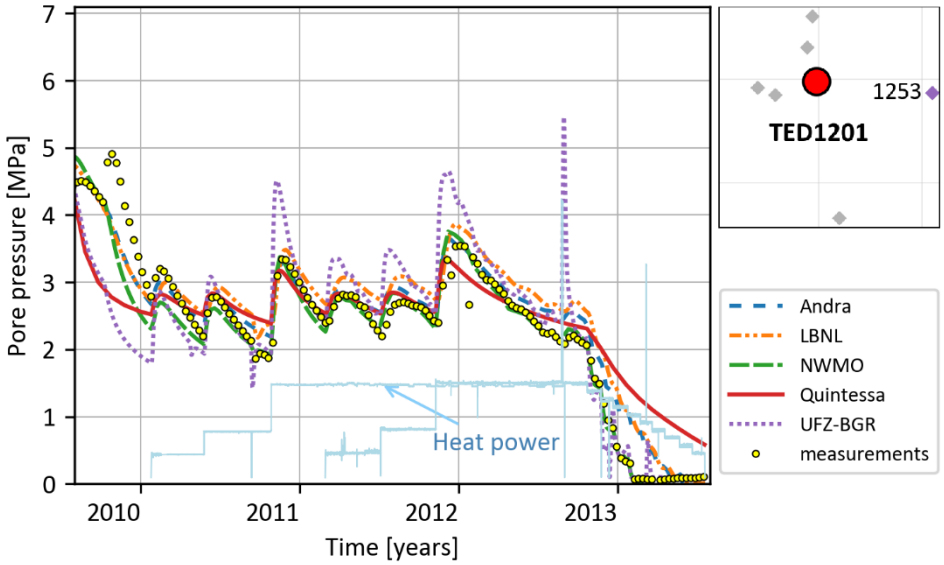


**Figure 26. Pressure evolution at sensor TED1253_PRE_01.**

The blind predictions of the ALC experimental results showed a good overall representation of evolution of the experiment, but did show a non-trivial deviation from the measurements (LBNL results shown as a representative example - Figure 27) with pore pressures only being well-represented parallel to the direction of bedding. Recalibrations were able to obtain better fits, including adjusting the EDZ representation and increasing the permeability anisotropy. This result appears to illustrate the impact of the spatial variability in the COx properties even over relatively short distances. . In addition, the stress and pore pressure fields around the micro-tunnel after its excavation were not well reproduced by the poro-elastic models probably leading to different hydraulic gradients during the heating.

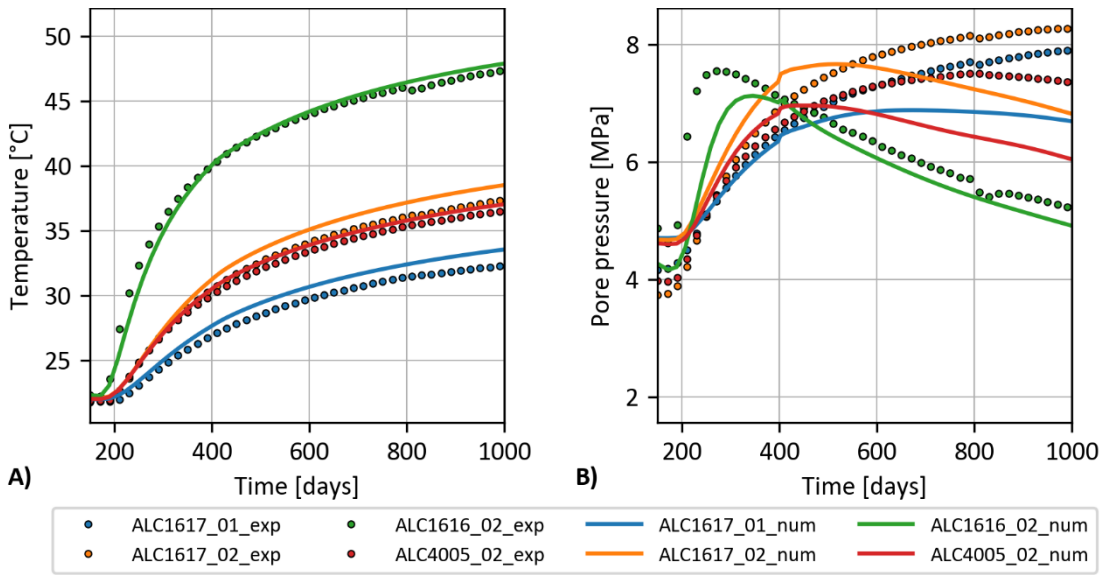


**Figure 27. Comparison of LBNL's numerical results measurements at selected sensors: (A) temperature and (B) pore pressure.**

Step 4, which involved THM modelling of one quarter of an entire repository with multiple galleries and disposal micro-tunnels (Figure 28) gave good and coherent results depending on the different geometrical assumptions made by the research teams. This builds confidence that large-scale repository models of this kind are tractable and robust, and can be used to predict temperatures and pore pressures. For some teams the simulation cases were sufficiently rapid to run that automated sensitivity analyses were possible investigating impacts of differing parameterization and geometrical assumptions (e.g., Figure 29)

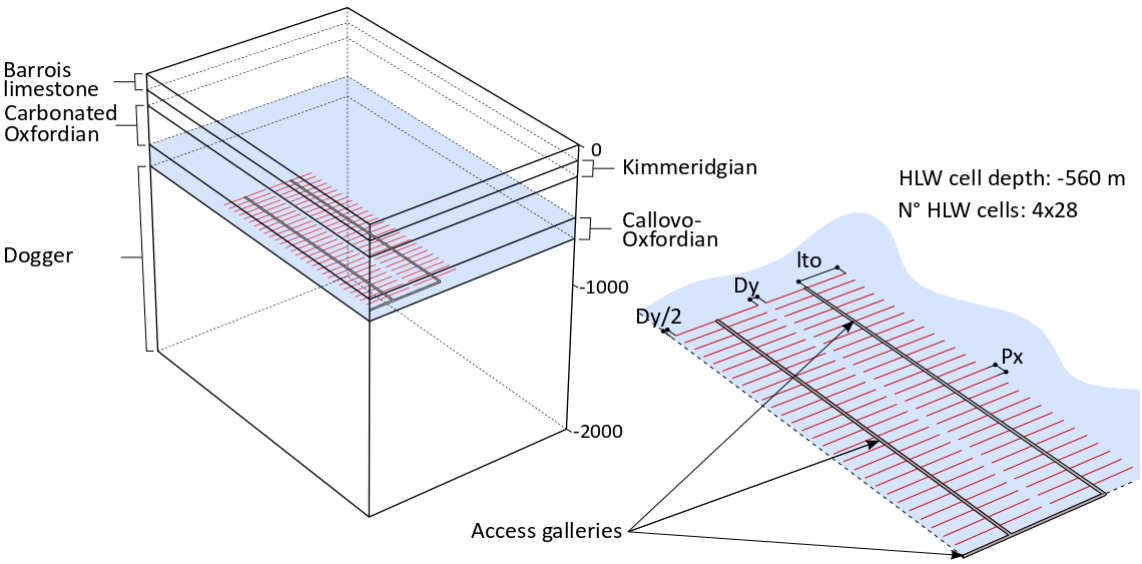


**Figure 28. Proposed configuration of a quarter of HLW repository.**

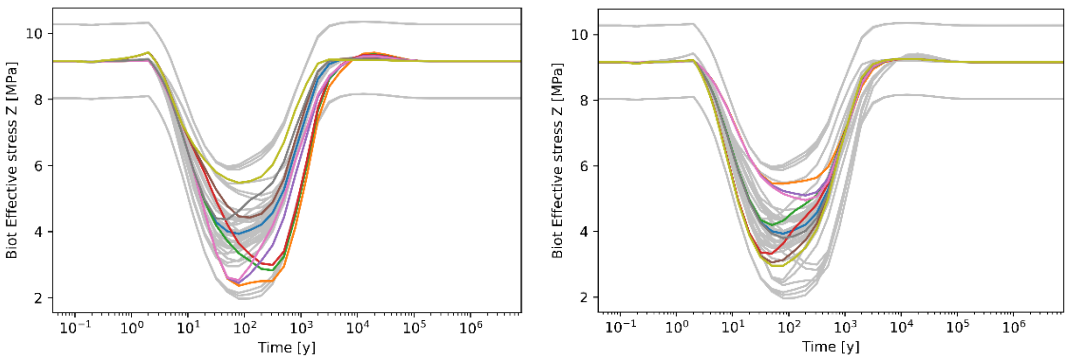


**Figure 29. Vertical Biot effective stress (compressive stress is represented with positive values) through time between HLW cells for 65 parameter sensitivity cases. Cases in which permeability (left) and Young's modulus (right) are altered and coloured. Other cases are plotted in grey.**

## 6.5 Key Outcomes

The modelling teams showed that the use of a thermo-poro-elastic model yielded satisfactory representations of the two in-situ heating experiments. A correct interpretation of the boundary conditions, equations of state for water, as well as finding permeability values keeping a anisotropy ratio consistent with respect to what is observed in the field, were essential for plausible and well-calibrated models.

Numerical modelling of the whole waste repository was also performed. Modeling teams had more freedom in order to set their models for repository-scale simulations, which led to different and original approaches. The assumptions and hypothesis enacted

in the different modelling approaches were verified by the inter-comparison of the numerical results. Step 4 thus provided a number of best practice guidelines for modelling large-scale deep geological repositories.

## 6.6 Outstanding Issues

In interpreting the field-scale in-situ experiments, the area of greatest uncertainty appeared to be in the correct representation of the EDZ created by the construction of the galleries and larger boreholes. The thermo-poro-elastic models are able to well represent the far field; however, they cannot, by their nature, properly represent the fractured area. These features were generally constructed by the teams using an empirical approach for EDZ properties rather than using a physics-based predictive model to generate the EDZs and evaluate related THM property changes. While the general THM behavior can be captured well without EDZs, if a detailed fully-predictive understanding of the impacts of construction damage is required, then more attention may be needed in future tasks to develop and compare empirical or physics-based approaches for EDZ prediction.

## 6.7 Future Work

Many of the aspects examined in Task E are being continued in DECOVALEX-2023. Task A in D-2023 is considering two experiments performed at the MHM URL where failure of the Callovo-Oxfordian is being provoked by rapid heating and gas injection. The approaches using in DECOVALEX-2019 Task E will be used and extended in this new task to address the additional processes and complexity for these new experiments. This will necessarily include an improved understanding of generation of damage and plasticity in the COx and may aid the understanding of EDZ generation.

# 7 Task F – Fluid Inclusion and Modelling in Tight Rock (FINITO)

## 7.1 Background and Motivation

Fluid inclusions are found within mineral crystals or along grain boundaries in evaporitic formations (Figure 30) as well as many sedimentary rocks and can migrate in the presence of thermal or hydro-mechanical gradients. For the disposal of radioactive waste, common host rock candidates such as clay and salt rock are considered tight with respect to fluid movement and such fluid inclusions are typically stagnant. However, they may become mobilized by a perturbation of the in situ state, which can occur due to excavation and geotechnical installations, the emplacement of heat-generating waste, or the generation of gas pressure. The migration of fluid inclusions can thus have important impacts on the long-term performance of a geologic repository for high-level radioactive waste disposal.

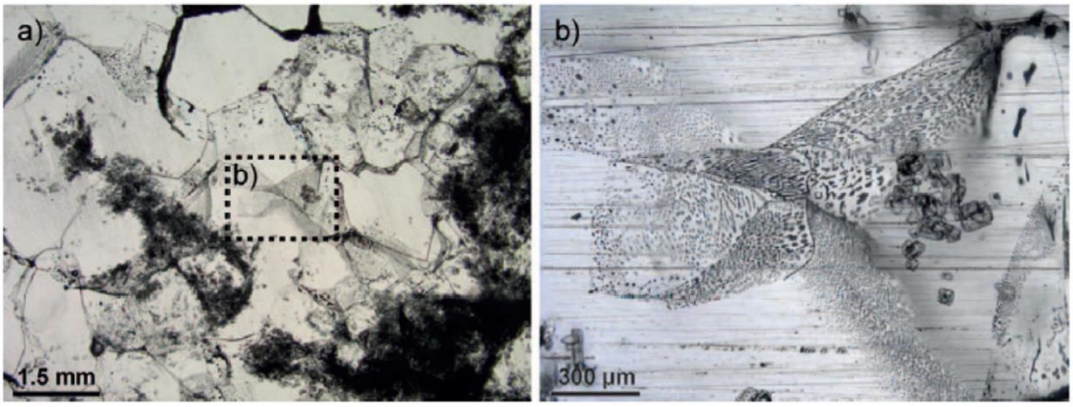


**Figure 30. Microscale image of fluid inclusions in rock salt (Thiemeyer et al., 2013).**

Within the DECOVALEX-2019 project, Task F was designed to investigate two aspects of fluid inclusion migration in rock salt under different boundary conditions: (a) altered hydro-mechanical conditions as a consequence of tunnel excavation or borehole drilling (Figure 31) and (b) coupled thermo-hydro-mechanical-chemical conditions during the heating period in the post-closure phase of a repository (Figure 32).

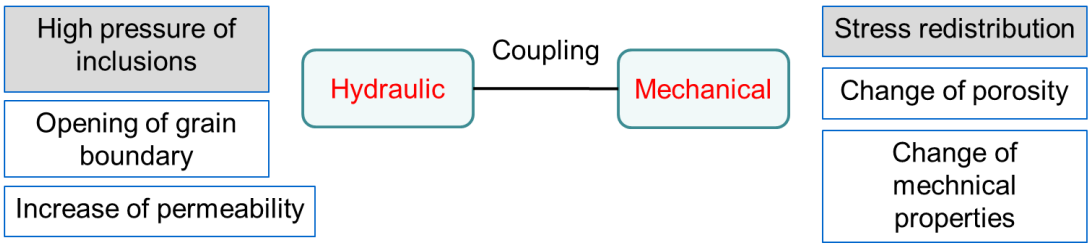


**Figure 31. Important process couplings for the fluid release by mechanical perturbations (drilling, excavation) during the construction phase.**

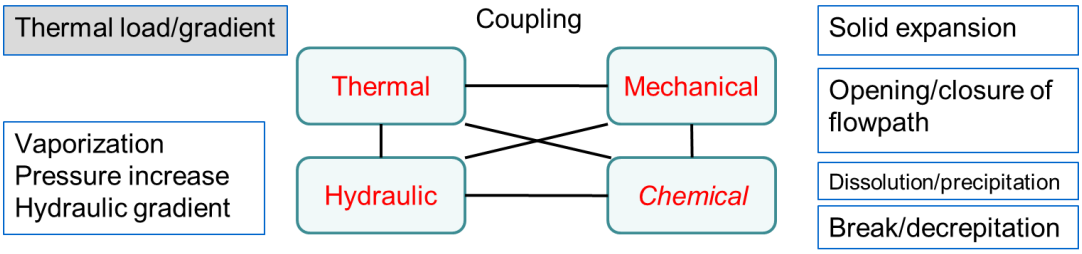


**Figure 32. Important process couplings for the migration of inclusions under a thermal/hydraulic gradient in the post-closure phase.**

## 7.2 Organization and Participation

In contrast to the classic approach of the DECOVLAEX project (benchmarking and test case comparison), this task was used as an innovation platform to understand the mechanisms of the fluid migration processes and potential implementation of those mechanisms in mathematical models. There were three research teams participating in the task:

- BGR (Federal Institute for Geosciences and Natural Research, Hannover, Germany)
- SNL (Sandia National Laboratories, Albuquerque, USA)
- UFZ/TUBAF (Helmholtz Centre for Environmental Research, Leipzig/Technische Universität Bergakademie Freiberg, Freiberg, Germany)

## 7.3 Task Approach and Selected Results

In both the operational (a) and post-closure phase (b), the important thermal, hydraulic and mechanical conditions were defined as a fluid flow driving mechanism, and used exiting tools or newly developed mathematical or numerical models to quantify the laboratory and field observations and measurements. To obtain a mechanistic understanding of possible physical processes driving fluid inclusion migration, a multi-scale modelling strategy was developed. Using a macro-scale model simulating an underground excavation procedure, the time-dependent deviatoric stress field around an opening due to the creep behavior of rock salt was determined (Figure 33), which was used as boundary conditions for micro-scale modelling (Shao et al. 2019).

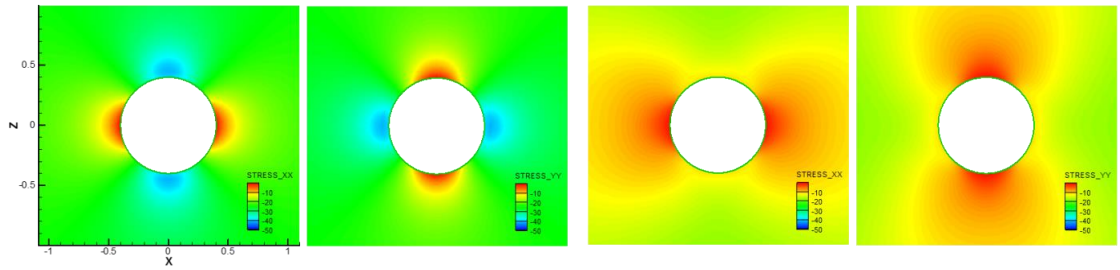


**Figure 33. Simulated horizontal and vertical stress distributions immediately after the excavation (left two) and 10 years later (right two),respectively.**

At the micro-scale, permeability changes due to strain deformation were determined using a coupled two-phase flow and elastoplastic model based on the effective stress concept. Pathway dilation along the halite grain boundary with an increased permeability of two orders of magnitude was estimated. This pathway dilation can be again simulated using a phase-field model. With this permeability, the measured pressure build-ups from an underground borehole can be simulated quite well taking into account the time-dependent damaged or disturbed zone caused by the coupling of mechanical (creep) and hydraulic (pressure release) processes (Shao et al. 2020) (Figure 34).

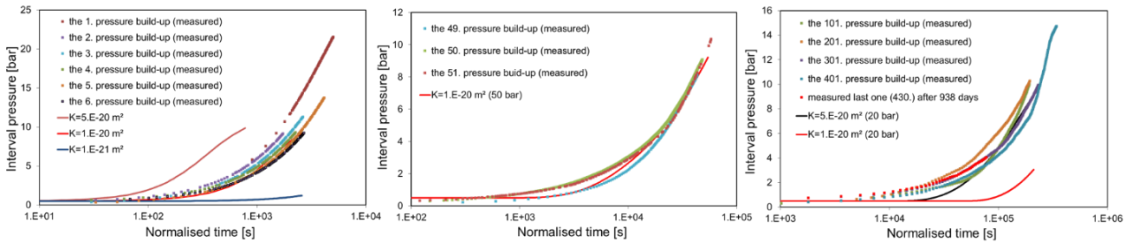


**Figure 34. Simulated with the FE code OpenGeoSys and measured pressure build-ups from a borehole with a high release rate: fluid inclusions located in the EDZ (l), in the EdZ (m) and in the undisturbed zone (r) with a later increased permeability in the Ed/DZ around the borehole**

In the post-closure phase of a repository, the stress state will evolve to the initial state due to the creep processes typically seen in rock salt if the backfill material has similar properties as the host rock. A micro-scale analysis of the characteristics of a coupled system was performed taking into account the migration of a single inclusion under a thermal gradient. The derived equation for calculating the velocity of inclusion migration describes the proportional relationship between the velocity and the size of the inclusion on the one hand, and the velocity and the temperature on the other.

## 7.4 Key Outcomes

Several conclusions can be drawn from the individual team analyses as well as from the interaction discussions held during workshops:

- Underground excavation leads to a time-dependent deviatoric stress state around the opening due to the creep behavior of salt.
- High inclusion pressures on the grain boundaries may open the boundary which forms a flow path with a permeability of two orders of magnitude higher than initially present.
- This pathway can remain temporarily open after the release of inclusions with a relatively high net permeability of $10^{-20}$ m². However this permeability is expected to be very localized and remains lower than other potential rock formations used for radioactive waste disposal.
- A liquid fluid inclusion moves towards a heating source at a velocity linearly proportional to the local thermal gradient.
- The velocity of inclusion migration also increases with the size of the inclusion.

## 7.5 Outstanding Issues

The work under Task F has been at a fundamental level and as such represents a work in progress. A coherent numerical solution to solve the time-dependent change of the damage or disturbed rock zone around an underground opening in rock salt has not been developed. However, given the interesting insights and the interesting relationships constructed, the obvious avenue is to attempt to apply the methodologies developed within a well-constrained experimental programme at different scales of interest. We hope that such a programme will be forthcoming in the near future and with this series of field observations, e.g. inflow of hydrocarbons or brine into boreholes can be modeled.

# 8 Task G - EDZ Evolution in Sparsely Fractured Competent Rock

## 8.1 Background and Motivation

The development of the excavation disturbed and excavation damage zone (EDZ) around deposition tunnels and holes is a target of attention in the development of radioactive waste disposal concepts. In crystalline host rock, understanding the formation of an EDZ is not required per se from a stability perspective, but mostly motivated by the fact that the formation of an EDZ will change the hydraulic properties of the rock mass in the vicinity of the excavations. Accordingly, there is a potential for increased fluid pathways parallel to the excavations. These induced pathways may act as transport channels for radionuclides. As the excavations might form a continuous network connected to the biosphere, the EDZ may also form a part of a pathway to the surface.

The formation of the EDZ and the associated change of rock mass permeability has been a continuous topic of research, not exclusive but prominently, in former DECOVALEX tasks (Liu et al. 2011; Wang et al. 2011; etc.). Many individual aspects have been covered within these studies, and also sequences of boundary condition changes have been analysed. However, the impact that the evolution of a repository for spent nuclear fuel, from construction to pre-closure and post-closure phases, may have on the EDZ development and the related transmissivity change has not been fully analysed. Further, it is unclear how rock mass transmissivity should be measured during the construction and operational phases and how these measurement relate to the conditions after closure of a repository.

Task G in DECOVALEX-2019 is primarily concerned with the evolution of transmissivity throughout the lifetime of a repository for radioactive waste, and in particular of spent nuclear fuel, in sparsely fractured and competent crystalline rock masses, and the representation of these processes via numerical simulation. The numerical simulations were to be evaluated for their suitability, and to be validated. Over the course of the work presented here, not only were transmissivity changes and the best approaches to simulate those changes examined, but also strategies were to be developed on how to monitor transmissivity changes *in situ*. Guidelines on what a control program and a monitoring system for a repository should include and be able to measure, and how this can be done in practice, was a key objective of the research project.

For more detail please see Meier and Backers (2020).

## 8.2 Organization and Participation

Three different teams from Seoul National University (SNU), Technical University of Liberec (TUL), and geomecon GmbH (GMC) participated in the task – the codes and general approaches to the interference test are given in Table 8.

**Table 8. Participants' code and general approach for Task F.**

| Team | Code | Approach (WP2) | Funding Organization |
|---|---|---|---|
| SNU | UDEC (WP1) and 3DEC (WP2) | Stress dependent fracture flow | SSM |
| TUL | COMSOL Multiphysics® | Fracture and matrix flow | SÚRAO |
| GMC | roxol (WP1 only) and COMSOL Multiphysics® | Fracture and matrix flow | SSM |

The Discrete Fracture Network (DFN) used by the modelling teams was generated by Clearwater Hardrock Consulting (USA).

The work programme consisted of the following work packages:

1. WP1: 2D benchmarking against a synthetic case
2. WP2: Modelling the TAS04 interference test (see information on TAS04 below)
3. WP3: Modelling transmissivity change due to DFN evolution

The work packages were divided into a series of different activities. WP1 and WP2 were completed, but WP3 was not attempted due to a lack of time and will be continued outside of DECOVALEX.

## 8.3 Experimental Data

This task was based on measurements performed in the TAS04 tunnel in Äspö (Sweden) by SKB as hydraulic interference tests (Ericsson et al. (2014), Ittner et al. (2014), Ittner et al. (2015), Ittner and Bouvin (2015), Ericsson et al. (2015)). The experimental setup included drilling 42 short drillholes into the tunnel floor with lengths ranging between 1 m and 2 m. Each was used as an injector hole while the neighboring drillholes served

as sites for monitoring pore pressure changes. These interference tests were used to determine the transmissivity of the rock and fractures and serve as a validation target to be modelled numerically within work package (WP) 2, which can be considered the main work package in Task G.

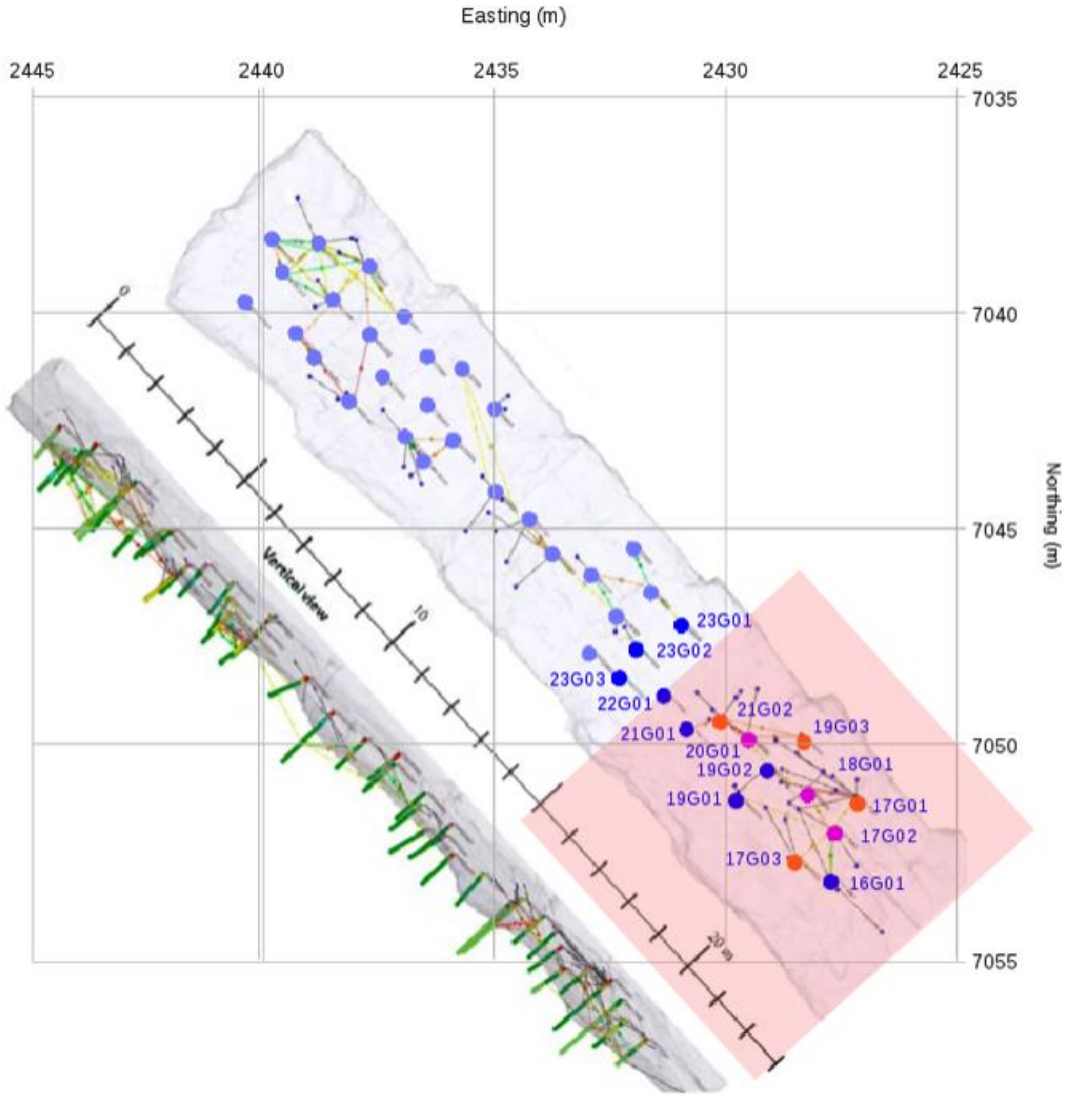


**Figure 35. Positions of drillholes in the floor of the TAS04 drift, plotted based on coordinates given in Appendix 1 of Ericsson *et al.* (2015). Colored dots show the proposed injection holes used for modelling of the interference tests (magenta) and registering hydraulic connections to these injection holes (orange), as well as differentiating those located in the selected test section of TAS04 (dark blue) relative to those outside this section (pale blue). The coordinate axes (easting and northing) are in the local Äspö system. This plot is superimposed on a reoriented version of Ericsson et al. (2015), Figure 8-19, with lines indicating the interpreted hydraulic connections between holes, and to leakage points in the tunnel floor (tiny blue dots). The lower left-hand part of the plot (below the diagonal scale) gives an orthogonal view of the drillholes to indicate their relative lengths and the depths of the**

**interpreted hydraulic connections. Note that the vertical scale in this view is exaggerated.**

## 8.4 Task Approach and Selected Results

WP1 considered 2D deterministic and stochastic fracture networks to be simulated and compared in 2D (Figure 36) with tightly controlled process models and parameterisation. While the results across teams were generally consistent and any differences clearly relatable to the implementation, clear differences were seen between the finite element method (FEM) implementations (COMSOL, roxol) and the discrete element method (DEM) implementation (UDEC) in some instances. In particular combining the stochastic and deterministic models produced significantly different results in the FEM methods, but not in the DEM model. The reasons for these differences have not been isolated and illustrate the potential for different results according to numerical method and modelling choices for such complex geometries, even when tightly prescribed.

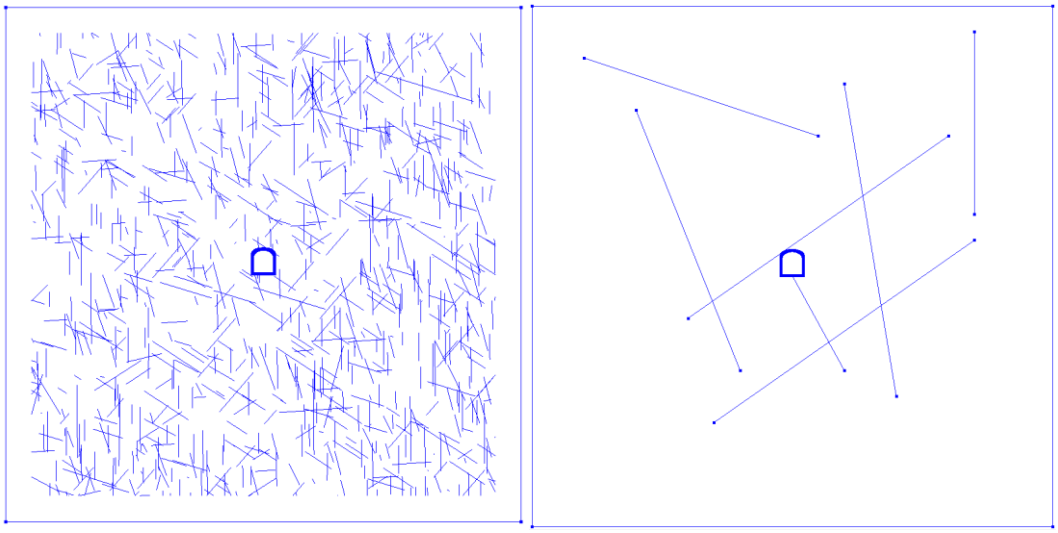

**Figure 36. Stochastic (left) and deterministic fracture networks for WP1.**

For WP2, the TAS04 experiment was examined by the teams, including available deterministic and DFN data. While ideally the fully available fracture information would be used, significant simplifications in the geometry had to be made for all the codes in order to make the problem tractable. In the case of COMSOL, very high numbers of fractures made the domain practically impossible to grid, while for 3DEC run times

became prohibitively large with a fine discretisation. An example mesh for COMSOL is shown in Figure 37.

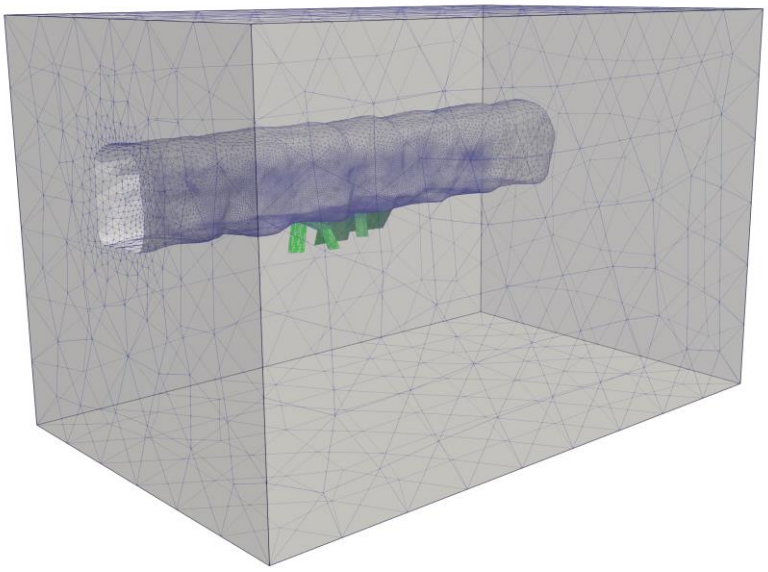

**Figure 37. Exampled discretization of the model geometry (except drillholes) showing a finer mesh in the area where the open fractures (green) are located as implemented by GMC in COMSOL Multiphysics®. Deterministic features only.**

While apparently plausible results could be generated from the models as increasingly complex tests were examined (Activities 2.1 – 2.3), unfortunately, none of the teams were successful in modelling the complex pressure response evident in the suite of interference tests that were conducted. Especially if an interference test caused high- and low-pressure responses in different neighboring drillholes, the numerical models were unable to accurately predict the pressure differences (Figure 38). This is particularly troublesome because it indicates that not all drillholes are connected to the interference test or that fracture flow towards one observation hole is blocked while it was open to another drillhole. An example for this behavior was the interference test where K04018G01 was the injector. In two neighboring drillholes K04017G01 and K04017G02, pressure responses with significant spread were observed despite both being connected by one fracture to the injection hole. This is probably related to channeling effects along the fractures since stress- and aperture-dependent models failed to predict this pressure response. Attempts to include channeling on the fractures have been not tested, further underlining the possibility of channeling along the fractures below the TAS04 tunnel.

The closest results to this have been observed in Activity 2.2 with $R^2$=0.66 and $R^2$=0.98 by GMC and TUL, respectively. Activity 2.1 and Activity 2.3 have much lower coefficients of determination.

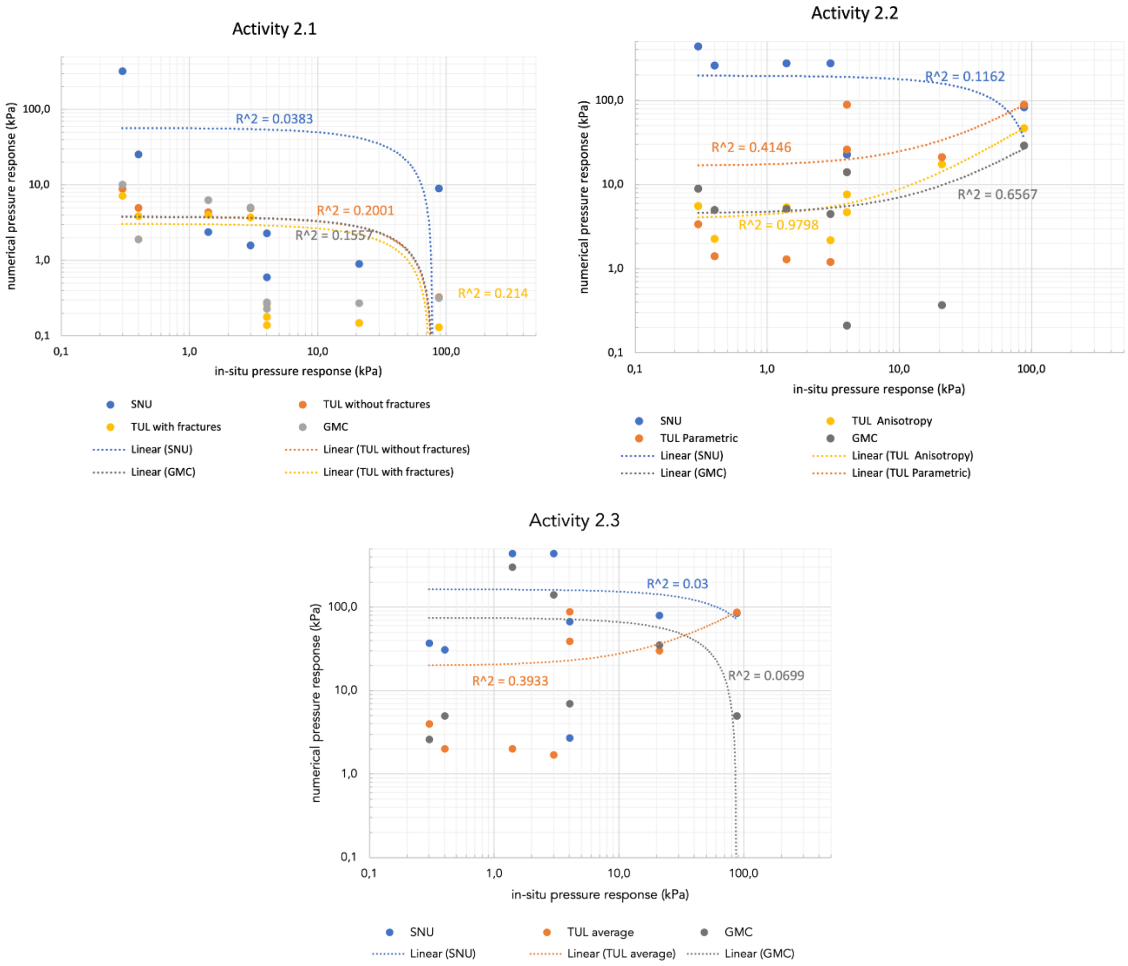


**Figure 38. Numerically modelled maximum pore pressure vs. maximum in-situ pore pressure from different interference tests obtained in Activity 2.1 – 2.3.**

## 8.5 Key Outcomes

While different approaches have been applied, it can be summarized that the codes were not able to predict all the in-situ pressure responses for the TAS04 experiment, particularly those with significant pressure differences in different observation holes, but were able to model the bulk inflow to the tunnel. Therefore, the numerical models may be not suitable for modelling such interference tests due to the fact that (a) not all provided data could be implemented within the modeling approaches used, (b) the provided data might be incomplete with reference to channels along the fractures (channeling), and (c) the differences between the regular and irregular tunnel geometry

induce stresses that differ from the in-situ stresses. This result illustrates the importance of having sufficient data to conceptualize and parameterize a model and that different models are often required for different modeling end-points for the same domain. In this case it is clear that the details of the interference tests were extremely challenging to match with the available models and data.

## 8.6 Outstanding Issues

To what extent WP3, which deals with post-closure features and processes like temperature increase, glaciation, and earthquakes, will yield reliable results is questionable. However, the results from this work package may indicate relative changes, e.g. whether the transmissivity in the excavation damage zone (EDZ) is going to increase or decrease during the post-closure processes. In this regard, the models applied to WP3 will bring about valuable insights and will enhance the prediction of the evolution of the repository after closure.

## 8.7 Future Work

WP3 is ongoing outside of DECOVALEX and results will be published in due course.

# 9 Concluding Remarks

DECOVALEX-2019 has explored some common themes across a range of tasks, yielding new insights but also encountering common issues that remain to be resolved. The tasks have examined four key areas between them:

- Novel representations of complex processes (Tasks A and F).
- Complexities flow and fracture representation in fractured rock (Tasks C and G).
- Complex hydro-mechanics with wider applications (Task B)
- THM processes in clays, focusing on issues associated with the mechanical representation (Tasks D and E).

## 9.1 Novel Representations of Complex Processes

Both Tasks A and F dealt with the extremely complex issues of highly non-linear fluid migration within very low permeability formations. Observed experimental behaviors are often strongly stochastic and therefore it can be very difficult to rationalize the core physical behavior (i.e. identify what experimental features are reproducible under different circumstances) and successfully interpret the experiments. In addition, the experimental setup can be very important in determining the result, hence careful representation of the experiment (e.g., the injector apparatus in Task A) can be key to building a successful model. In this context, the DECOVALEX working model of close integration between experiment and modeling is an important one. For example, the model comparison in Task A was coordinated by the very scientist who conducted the series of experiments.

In the case of Task A, the primary concern was advection of pressurized gas in compacted bentonite, while Task F mainly considered migration of inclusions in salt formations. While superficially quite distinct, there are a number of commonalities, and indeed the SNL research team used similar approaches in both tasks to characterize and represent the experiment.

For Task A, it was shown that conventional two-phase flow approaches are largely inadequate to represent the system in a convincing fashion, taking into account all the known features of the experimental results (e.g. very low gas saturations at breakthrough). Hence the inclusion of implicit or explicit features to represent the dilation process is essential. Similarly for Task F, explicit treatment of fluid migration

along the halite grain boundaries, also by a dilation process under strongly deviatoric stress conditions, was found to be a good representation of salt inclusion migration.

Both tasks have illustrated the importance of micro-scale control on macro-scale phenomena and novel approaches for bringing the micro-scale understanding into the meso- and macro-scale have been put forward.

## 9.2 Complexities of Fracture Representation

Tasks C and G both dealt with the problem of interpreting groundwater flows and (in the case of Task C) transport within discrete fracture networks (DFNs). This is an area of long-standing study within DECOVALEX and the tasks have encountered many of same issues, albeit from a different perspective. Both tasks illustrated that producing models that can successfully represent net tunnel inflows is possible with plausible DFN based on geological observation, with some calibration and some teams using an equivalent continuum porous medium (EPCM) approach.

However, both tasks struggled when looking at more complex aspects of the problem. In the case of Task C, successfully modelling the wide range of observed chloride concentrations in the tunnel was particularly problematic. Producing a convincing representation of the transport required manual intervention in the DFN/EPCM to create large-scale heterogeneity to allow the excavated tunnel to connect to vertically distant higher and lower concentrations of chloride. Task G showed a similar issue at a much smaller scale, whereby the interference tests in the TAS04 experiment were very hard to interpret and model when using intersection of identified planar fracture surfaces identified in the EDZ. Both tasks concluded that channelization with the fracture network could be the cause of the difficulties in modeling the observations, nothing that large scale heterogeneities in the DFN network for Task C could also be a factor.

## 9.3 Complex Hydro-Mechanics with Wider Applications

For Task B, the problem was focused on a single fault-zone in an argillite rather than a DFN system in a crystalline potential host rock. Here the work focused on the numerical issues of a good representation of an extremely well-characterized fault system that was stimulated using fluid injection. The highly non-linear nature of the hydro-mechanical response meant that different numerical methods were found to have different

strengths and weaknesses. This necessitated different modelling strategies and conditioning of the models with respect to the known data, depending on the numerical approach. Nonetheless, after considerable effort, consistent and coherent results for the experiment have been produced. A useful next step to build confidence would be predictive studies of small-scale fault reactivation. This task is also of interest outside of the radioactive waste management arena, being of direct relevance to other sub-surface geo-engineering applications (e.g. geothermal, underground gas/air storage, oil and gas etc.)

## 9.4 THM Processes in Clays

Task D and E both considered THM processes in clays or clay-based materials such as bentonite, albeit from different perspectives. Task E demonstrated that good blind predictions of pore-pressure and temperature can be obtained for heat-generating disposal analogues using heat diffusion and conventional elastic poro-mechanics. There was some evidence of surprising local heterogeneity in the Callovo-Oxfordian clay which meant some recalibration was required when moving between experiments. This work clearly illustrated the impact of variability and heterogeneity on pore pressure. The teams were also able to use their models in an upscaled mode to represent the whole repository, and use these models to investigate the sensitivity of uncertainty and variability on key metrics (pore pressure and implied effective stress) that could impact the safety case. In understanding the details of the experiments, it was clear that the development of the EDZ, and the resulting effective hydraulic and mechanical properties of the EDZ, were important to calibrate the models to the observations. This remains a complex exercise and differing approaches were taken by the teams, but no fully mechanistic model was used by any team. While the task was a clear success, the treatment of mechanical damage and the resulting change in the argillite properties, remains an area of significant uncertainty.

Task D was focused on compacted and pelleted bentonite used as a buffer material in two very different experiments. While teams were able to obtain good agreement with the measured thermal and hydraulic responses, a complete representation of the plastic mechanical deformation – in this case focused on the homogenization of the bentonite during heating and resaturation – remains challenging. This was not helped by non-trivial uncertainties in some of the in-situ data. It was noted that highly simplified mechanical models could be used in some circumstances, depending on the modelling objectives.

Both tasks have encountered similar issues in terms of treatment of the plasticity of clays (Task D – homogenization, Task E – damage), albeit from different perspectives. This perhaps indicates the direction for future work in argillites from a coupled processes perspective. Indeed, a task on rock failure in the Callovo-Oxfordian due to gas and water overpressure will form part of the next phase of DECOVALEX.

## 9.5 Overall Comments

For DECOVALEX-2019, despite the challenges mentioned above, significant progress was achieved by research teams of all tasks, some of which were dealing with extremely complex processes. Modeling teams adopted advanced modelling approaches using different numerical methods and computer codes and were generally able to achieve good agreement, both with the experimental observations and with alternative modeling approaches. In cases where differences remained, task leads and modeling teams made an effort in isolating the reasons for them and discussed what could to be done to improve. Overall, the achievements and outstanding issues obtained from the seven tasks formed a good step forward for better understanding of the scientific/technical issues of importance for safe geological disposal of radioactive wastes in different host rocks, with complex geological conditions and increasing environmental challenges.

The achievements of the DECOVALEX-2019 Project are demonstrated by a large number of planned and published scientific publications in international journals and conferences/symposiums, as described in the six Task reports (and one journal paper that acts as the task report for Task F) and a very well attended "DECOVALEX-2019 Symposium on Coupled Processes in Radioactive Waste Disposal and Subsurface Engineering Applications". 31 papers have been submitted for a virtual special issue in the International Journal of Rock Mechanics and Mining Sciences with many accepted and in publication at the time of writing this executive summary. We are also pleased with a good level of work being presented at a wide range of international conferences and several published papers outside of the virtual special issue.

The coupled-processes research of DECOVALEX will be continued in the next phase of the project (DECOVALEX-2023) which will aim to take and develop much of the work that has been produced during the current phase. In particular, direct extensions of Task A and E are planned and include many more challenging aspects. DECOVALEX-2023 will also, for the first time, feature a task on radioactive waste disposal in bedded salt, featuring a salt heater test conducted in the US Department of Energy's Waste Isolation

Pilot Plant (WIPP). And it will comprise a task focusing on the models, methods, and software used for performance assessment or safety assessment for deep geologic repositories, which are often built on the knowledge gained from coupled processes models. As ever, the emphasis of the tasks will be on radioactive waste management, but much of the work planned will be have direct bearing on a wide range of geo-engineering applications.

# 10 Acknowledgements

DECOVALEX is an international research project comprising participants from industry, government and academia, focusing on development of understanding, models and codes in complex coupled problems in sub-surface geological and engineering applications; DECOVALEX-2019 is the current phase of the project. The authors appreciate and thank the DECOVALEX-2019 Funding Organizations Andra, BGR/UFZ, CNSC, US DOE, ENSI, JAEA, IRSN, KAERI, NWMO, RWM, SÚRAO, SSM and Taipower for their financial and technical support of the work described in this report. The statements made in the report are, however, solely those of the authors and do not necessarily reflect those of the Funding Organizations.

# 11 References


Daniels K.A. and Harrington J.F. 2017. The Response of Compact Bentonite during a 1D Gas Flow Test. British Geological Survey Open Report, OR/17/067. 19pp.

ENRESA. 2000. FEBEX project. Full-scale engineered barriers experiment for a deep geological repository for high level radioactive waste in crystalline host rock. Final report. Publicación Técnica 1/2000, ENRESA, Madrid.

Gens A. 2020. DECOVALEX-2019 – Task D Final Report. LBNL Report LBNL-2001267.

Graupner B, Rutqvist J and Gugliemi Y. 2020. DECOVALEX-2019 – Task B Final Report. LBNL Report LBNL-2001263.

Guglielmi, Y., Birkholzer, J., Rutqvist, J., Jeanne, P., Nussbaum, C. (2017). Can Fault Leakage Occur Before or Without Reactivation? Results from an in Situ Fault Reactivation Experiment at Mont Terri, Energy Procedia, Volume 114, Pages 3167-3174, ISSN 1876-6102, https://doi.org/10.1016/j.egypro.2017.03.1445.

Harrington J.F. and Horseman S.T. 2003. Gas migration in KBS-3 buffer bentonite: Sensitivity of test parameters to experimental boundary conditions. Report TR-03-02. Svensk Kärnbränslehantering AB (SKB), Stockholm, Sweden.

Harrington J.F., Graham C.C., Cuss R.J. and Norris S. 2017. Gas network development in a precompacted bentonite experiment: Evidence of generation and evolution in Applied Clay Science. 147, 80-89. DOI: 10.1016/j.clay.2017.07.005.

Liu Q., Wu Y., Liu B. 2011. Discrete element analysis of effect of stress on equivalent permeability of fractured rockmass, Yanshilixue Yu Gongcheng Xuebao/Chinese Journal of Rock Mechanics and Engineering, 30(1), 176-183.

Marschall, P., Horseman, S. and Gimmi, T. 2005. Characterisation of gas transport properties of the Opalinus Clay, a potential host rock formation for radioactive waste disposal. Oil Gas Sci. Technol., 60, 1, 2, 2005

Mayor J.C. et al. 2007. Engineered barrier emplacement experiment in Opalinus Clay for the disposal of radioactive waste in underground repositories. in P. Bossart and C. Nussbaum (editors) Mont Terri Project - Heater Experiment, Engineered Barriers Emplacement and Ventilation Tests (p. 115-179). Rep. Swiss Geol. Survey No. 1.

Martin, C.D. and Lanyon, G.W. 2003. Measurement of in-situ stress in weak rocks at Mont Terri Rock Laboratory, Switzerland. International Journal of Rock Mechanics and Mining Sciences, 40(7-8). 1077-1088

Meier, T. and Backers, T. 2020. DECOVALEX-2019 – Task G Final Report. LBNL Report LBNL-2001266.

Plua C., Vitel M., Seyedi D.M. and Armand G.. 2020. DECOVALEX-2019 – Task E Final Report. LBNL Report LBNL-2001265.

Shao H., Wang Y., Kolditz O. Nagel T. and Bruning T. 2019. Approaches to multi-scale analyses of mechanically and thermally-driven migration of fluid inclusions in salt rocks. Physics and Chemistry of the Earth, 113, p1-13. https://doi.org/10.1016/j.pce.2019.07.003

Tamayo-Mas E. and Harrington J.F. 2020. DECOVALEX-2019 – Task A Final Report. LBNL Report LBNL-2001262.

Iwatsuki T. 2020. DECOVALEX-2019 – Task C Final Report. LBNL Report LBNL-2001264.

Thiemeyer, N., Pusch, M., Hammer, J. & Zulauf, G. 2013. Quantification and 3D visualisation pf pore space in Gorleben rock salt: Constraints from CT imaging and microfabrics, Z. Dt. Gers. Geowiss, Dec. 2013.

Wang W., Rutqvist J., Görke U.-J., Birkholzer J.T., Kolditz O. (2011). Non-isothermal flow in low permeable porous media: a comparison of Richards' and two-phase flow approaches, Environmental Earth Sciences, Vol. 62(6), p. 1197-1207, DOI:10.1007/s12665-010-0608-1